Medicinal Chemistry Research (2019) 28:2050–2066
https://doi.org/10.1007/s00044-019-02435-0

MEDICINAL CHEMISTRY RESEARCH

ORIGINAL RESEARCH



# Antimalarial, antiproliferative, and apoptotic activity of quinoline-chalcone and quinoline-pyrazoline hybrids. A dual action

Jaime E. Charris[1] · Melina C. Monasterios[1] · María E. Acosta[1] · Miguel A. Rodríguez[1] · Neira D. Gamboa[1] · Gricelis P. Martínez[2] · Héctor R. Rojas[3] · Michael R. Mijares[2,3] · Juan B. De Sanctis[3,4]

Received: 5 July 2019 / Accepted: 29 August 2019 / Published online: 24 September 2019


## Abstract

A series of quinoline-chalcone *(E)*-1-[3 or 4-(7-chloroquinolin-4-ylamino) phenyl]-3-(phenyl substituted) prop-2-ene-1-one (**4**, **5**), and quinoline-pyrazoline hybrids 7-Chloro-*N*-[3 or 4-(4,5-dihydro-5-(phenyl-substituted)-1H-pyrazol-3-yl] phenyl) quinoline-4–amine (**6**, **7**) were synthesized with the aim of achieving an antimalarial and anticancer dual action. Most of the compounds showed significant inhibition (%>80) of β-hematin formation. The existing structures were tested in vivo as potential antimalarials in mice infected with *P. berghei* ANKA, chloroquine susceptible strain. Some of the compounds exhibited antimalarial activity comparable to that of chloroquine. Moreover, the compounds induce cell death on two human cancer cell lines (Jurkat E6.1 and HL60) without affecting the primary culture of human lymphocytes. Flow cytometry analysis confirmed the increase in apoptotic cell death after 24 h. Based on the structural analysis, these quinoline hybrids represent new compounds potentially useful for malaria end leukemia treatments.

**Keywords** Anticancer · Antimalarial · Apoptosis · Chalcone · Pyrazoline · Quinoline

## Introduction

Malaria is a multifaceted tropical disease that has been transmitted by the bite of female Anopheles mosquitoes (Plewes et al. 2019). Five species are responsible for the infection *Plasmodium falciparum*, *vivax*, *ovale*, *malariae*, and lastly *Knowlesi* (Plewes et al. 2019). According to the World Malaria Report (World Health Organization 2018), there is an increase in malaria cases, more than 2 million from 2016 (217 million cases) to 2017 (219 million cases), the estimated number of malaria deaths stood at 435,000 in 2017. The increase is due to the lack of proper controls in several countries (Grillet et al. 2019). It is concluded that new approaches for treatment are urgently needed. Malaria incidence can be decreased through vector control; however, resistance to insecticides and chemotherapeutics have difficulted the task (WHO 2018; Grillet et al. 2019).

Cancer has been defined as a severe disease caused by the uncontrolled growth of cells, tissue destruction, and death. It is the second principal cause of death worldwide after ischemic heart disease and stroke, 17 million new cases and 9.6 million deaths in 2018. Moreover, 33% of the cancers are linked to tobacco exposure (Cancer Research UK 2018).

Several studies have suggested a possible interaction among parasites and cancer (Faure 2016; Phillips et al. 2017; Maji 2018). Several antimalaria agents, like chloroquine (CQ) and its derivatives, have been used in cancer chemotherapy (Faure 2016; Phillips et al. 2017; Maji 2018). One of the mechanisms postulated is Bcl-2 inhibition (Strasser and Vaux 2018), as well as its effect in autophagy (Nordstrøm et al. 2015; Bhat et al. 2018; Levy et al. 2017). Several other compounds synthesized by our group have shown antimalarial and

**Supplementary information** The online version of this article (https://doi.org/10.1007/s00044-019-02435-0) contains supplementary material, which is available to authorized users.

✉ Jaime E. Charris
jaime.charris@ucv.ve

[1] Organic Synthesis Laboratory, Biochemistry Unit, Faculty of Pharmacy, Central University of Venezuela, 47206, Los Chaguaramos 1041-A, Caracas, Venezuela

[2] Biotechnology Unit, Faculty of Pharmacy, Central University of Venezuela, 47206, Los Chaguaramos 1041-A, Caracas, Venezuela

[3] Institute of Immunology, Faculty of Medicine, Central University of Venezuela, 50109, Los Chaguaramos 1050-A, Caracas, Venezuela

[4] Institute of Molecular and Translational Medicine, Faculty of Medicine, Palacky University, Hněvotínská 1333/5, 779 00 Olomouc, Czech Republic

cytotoxic effects on cancer cells (Rodrigues et al. 2012; Romero et al. 2018, 2019). Hemozoin formation was shown to be inhibited by CQ in the parasite food vacuole (Egan and Ncokazi 2005; Joshi and Viswanathan 2006). Artemisinin (AT) also targets the parasite vacuole by binding to the heme and impede the parasites detoxification of β-hematin generating the insoluble toxic hemozoin (Weissbuch and Leiserowitz 2008; Fong and Wright 2013). Likewise, AT and semisynthetic derivatives activate apoptotic pathways in several tumor cell lines. The pathways involve loss of mitochondrial membrane potential, mitochondrial release of cytochrome c, decrease in Bcl-2 and Bcl-XL, increase in Bak/Bax, and activation of caspases 9 and 3 (Handrick et al. 2010; Xu et al. 2011; Zhou et al. 2012). Heme, apparently activated AT, and involve mitochondrial induced cytotoxicity (Meshnick et al. 1991; O'Neill et al. 2010). It follows then that these compounds offer an important therapeutic option for both diseases. Since the target affected, differ resistance mechanism may vary. One of the options is the combination of quinoline nucleus of with chalcones. The aim is to increase the biological activity of the merged compounds as compared to the single structure (Rodrigues et al. 2012; Zhang et al. 2013; Mahajan et al. 2007; Ferrer et al. 2009; Kumar et al. 2010; Lombard et al. 2011; Pretorius et al. 2013; Insuasty et al. 2013; Smit and N'Da 2014; Ratchanok et al. 2014; Ramírez-Prada et al. 2017; Alegaon et al. 2017).

In an effort to develop improved compounds with dual action antimalarial and anticancer, we report the synthesis and evaluation of the antimalarial, cytotoxic and pro-apoptotic activity of quinoline-chalcone and quinoline-pyrazoline hybrids and proposed some structural features required for a critical biological dual action.

## Materials and methods

### Chemical

NMR spectra were recorded on a JEOL Eclipse™ 270 MHz for $^{1}$H-NMR and at 67.9 MHz for $^{13}$C-NMR using $CDCl_3$ or $DMSO_{d6}$, and are reported in ppm downfield from the residual $CHCl_3$ or DMSO. Elemental analyses were obtained using a Perkin Elmer 2400 CHN elemental analyses. The results were within ±0.4% of the predicted values. A Nicolet™ IS5 FT-IR (ID3 Zn-Se) spectrophotometer was used to determine the IR spectra. A Thomas micro hot stage device was used to determine the melting points (mp). All organic products or solvents (from Sigma-Aldrich Group, USA) were used directly or distilled and dried in the usual manner, respectively. Thin-layer chromatography was carried out on Merck silica F254 0.255–mm plates, and spots were visualized by UV fluorescence at 254 nm. Compounds **2** and **3** have previously been synthesized (Ferrer et al. 2009; Insuasty et al. 2013; Romero et al. 2015).

### General procedure for the synthesis of (E)-1-[3 or 4-(7-chloroquinolin-4-ylamino) phenyl]-3-(phenyl-substituted) prop-2-en-1-one (4, 5)

In a glass bottle with a screw cap with magnetic stirring, 150 mg (0.51 mmol, 1 equiv.) of 7-Chloro-4-(3 or 4–acetylphenyl) amino quinoline (**2** or **3**) were placed, the respective aldehyde (0.56 mmol, 1.1 equiv.), a pellet of potassium hydroxide and 8 mL of methanol, the combination was agitated at room temperature for 96–120 h, obtaining a solid which was sieved and washed with water, diethyl ether, and recrystallized from ethanol.

#### (E)-1-[3-(7-chloroquinolin-4-ylamino)phenyl]-3–p-tolylprop-2-en-1-one (4a)

Yield: 46.38%. mp: 297–298 °C. IR (KBr pellet cm$^{-1}$): 3351 (NH), 1645 (C=O). $^{1}$H NMR (270 MHz, δ ppm, DMSO$d_6$): 9.26 (brs, 1H, NH), 8.48 (d, H2, $J = 5.2$Hz), 8.41 (d, 1H, H5, $J = 9.2$Hz), 8.03 (d, 1H, H8, $J = 1.9$ Hz), 7.55–7.93 (m, 9 H, H6, H2′, H4′, H5′, H6′, Ha, Hb, H2″, H6″), 7.23 (d, 2H, H3″, H5″, $J = 7.9$ Hz), 6,98 (d, 1H, H3, $J = 5.2$Hz), 2.31 (s, 3H, $CH_3$). $^{13}$C NMR (67.9 MHz, δ ppm): 21.7, 102.8, 119.1, 121.6, 122.4, 124.6, 125.0, 125.7, 127.1, 128.3, 129.6, 130.1, 130.5, 132.5, 134.6, 139.5, 141.4, 141.5, 144.0, 148.1, 150.2, 152.6, 189.42. Anal. calcd. for $C_{25}H_{19}ClN_2O$: (%) C, 75.28; H, 4.80; N, 7.02. Found: (%) C, 75.29; H, 4.83; N, 7.23.

#### (E)-1-[3-(7-chloroquinolin-4-ylamino)phenyl]-3-(2,3-dimethoxyphenyl)prop-2-en-1-one (4b)

Yield: 45.08%. mp: 129–131 °C. IR (KBr pellet cm$^{-1}$): 3350 (NH), 1647 (C=O). $^{1}$H NMR (270 MHz, δ ppm, DMSO$d_6$): 9.31 (brs, 1H, NH), 8.51 (d, 1H, H2, $J = 5.2$Hz), 8.44 (d, 1H, H5, $J = 9.2$Hz), 8.04 (d, 1H, H8, $J = 1.9$ Hz), 7.98 (d, 1H, Ha, $J = 15.8$ Hz), 7.84–7.97 (m, H, H2′, H4′, H6″), 7.58–7.66 (m, 4H, H6, H5′, H6′, Hb), 7.14–7.16 (m, 2H, H4″, H5″), 7.02 (d, 1H, H3, $J = 5.2$Hz), 3.83 (s, 3H, $OCH_3$), 3.79 (s, 3H, $OCH_3$). $^{13}$C NMR (67.9 MHz, δ ppm): 56.4, 61.6, 102.8, 115.7, 119.0, 119.8, 122.3, 123.5, 124.5, 124.9, 125.0, 125.8, 127.2, 128.3, 128.7, 130.5, 134.6, 138.9, 139.40, 141.5, 148.1, 148.9, 150.2, 152.6, 153.4, 189.6. Anal. calcd. for $C_{26}H_{21}ClN_2O_3$: (%) C, 70.19; H, 4.76; N, 6.30. Found: (%) C, 70.25; H, 4.80; N, 6.41.

#### (E)-1-[3-(7-chloroquinolin-4-ylamino)phenyl]-3-(2,4-dimethoxyphenyl)prop-2-en-1-one (4c)

Yield: 43.08%. mp: 129–131 °C. IR (KBr pellet cm$^{-1}$): 3355 (NH), 1660 (C=O). $^{1}$H NMR (270 MHz, δ ppm,

DMSO$d_6$): 9.30 (brs, 1H, NH), 8.52 (d, 1H, H2, $J = 5.2$Hz), 8.45 (d, 1H, H5, $J = 8.9$ Hz), 8.02 (s, 1H, H8), 8.00 (d, 1H, Ha, $J = 15.6$ Hz), 7.91–7.94 (m, 2H, H2′, H4′), 7.76 (d, 1H, Hb, $J = 15.6$ Hz), 7.59–7.65 (m, 3H, H6, H5′, H6′), 7.03 (d, 1H, H3, $J = 5,2$Hz), 6.65 (m, 2H, H3″, H5″), 3.91 (s, 3H, $OCH_3$), 3.85 (s, 3H, $OCH_3$). $^{13}$C NMR (67.9 MHz, δ ppm): 56.1, 56.2, 99.0, 102.8, 107.0, 116.5, 119.1, 119.9, 122.2, 124.3, 125.0, 125.7, 126.7, 128.3, 130.4, 130.9, 134.6, 139.7, 139.8, 141.6, 148.1, 150.3, 152.6, 163.5, 189.5. Anal. calcd. (%) $C_{26}H_{21}ClN_2O_3$: C, 70.19; H, 4.76; N, 6.30. Found: C, 69.99; H, 4.76; N, 6.51.

#### (E)-1-[3-(7-chloroquinolin-4-ylamino)phenyl]-3-(2,5-dimethoxyphenyl)prop-2-en-1-one (4d)

Yield: 44.14%. mp: 205–206 °C. IR (KBr pellet cm$^{-1}$): 3424 (NH), 1658. $^1$H NMR (270 MHz, δ ppm, DMSO$d_6$): 9.32 (brs, 1H, NH), 8.51 (d, 1H, H2, $J = 5.2$Hz), 8.44 (d, 1H, H5, $J = 9.2$Hz), 8.06 ((d, 1H, Ha, $J = 15.6$ Hz), 8.04 (s, 1H, H8), 7.87–7.98 (m, 3H, H2′, H4′, H6″), 7.55–7.70 (m, 4H, H6, H5′, H6′, Hb), 7.03–7.05 (m, 3H, H3, H3″, H4″), 3.84 (s, 3H, $OCH_3$), 3.78 (s, 3H, $OCH_3$). $^{13}$C NMR (67.9 MHz, δ ppm): 56.3, 56.7, 102.8, 113.3, 113.6, 118.8, 119.1, 122.3, 122.6, 124.0, 124.6, 125.0, 125.7, 127.0, 128.3, 130.5, 134.6, 139.2, 139.5, 141.5, 148.1, 150.2, 152.6, 153.3, 153.8, 189.6. Anal. calcd. (%) $C_{26}H_{21}ClN_2O_3$: C, 70.19; H, 4.76; N, 6.30. Found: C, 69.99; H, 4.76; N, 6.51.

#### (E)-1-[3-(7-chloroquinolin-4-ylamino)phenyl]-3-(3,4-dimethoxyphenyl)prop-2-en-1-one (4e)

Yield: 41.30%. mp: 179–181 °C. IR (KBr pellet cm$^{-1}$): 3430 (NH), 1657 (C=O). $^1$H NMR (270 MHz, δ ppm, DMSO$d_6$): 9.30 (brs, 1H, NH), 8.51 (d, 1H, H2, $J = 5.2$Hz), 8.44 (d, 1H, H5, $J = 9.2$Hz), 8.03 (s, 1H, H8), 7.77 (d, 1H, Ha, $J = 15.6$ Hz), 7.75–7.84 (m, 2H, H4′, H6′), 7.72 (d, 1H, H2′, $J = 1.9$ Hz), 7.53–7.69 (m, 4H, H6, H5′, Hb, H5″), 7.40 (d, 1H, H6″, $J = 8.4$ Hz), 7.02 (m, 2H, H3, H2″), 3.84 (s, 3H, $OCH_3$), 3.81 (s, 3H, $OCH_3$). $^{13}$C NMR (67.9 MHz, δ ppm): 56.2, 56.3, 102.7, 111.4, 112.1, 119.0, 120.2, 122.3, 124.6, 125.0, 125.8, 127.0, 128.0, 128.3, 130.4, 134.6, 139.7, 141.4, 145.5, 148.1, 149.6, 150.2, 152.0, 152.6, 189.3. Anal. calcd. (%) $C_{26}H_{21}ClN_2O_3$: C, 70.19; H, 4.76; N, 6.30. Found: C, 70.21; H, 4.78; N, 6.43.

#### (E)-1-[3-(7-Chloroquinolin-4-ylamino)phenyl]-3-(3,5-dimethoxyphenyl)prop-2-en-1-one (4f)

Yield: 50.30%. mp: 200–201 °C. IR (KBr pellet cm$^{-1}$): 3360 (NH), 1645 (C=O). $^1$H NMR (270 MHz, δ ppm, DMSO$d_6$): 9.26 (brs, 1H, NH), 8.46 (d, 1H, H2, $J = 5.2$Hz), 8.39 (d, 1H, H5, $J = 9.2$Hz), 8.01 (s, 1H, H8), 7.86–7.96 (m, 3H, H2′, H4′, Ha), 7.65 (d, 1H, Hb, $J = 15.6$ Hz), 7.54–7.67 (m, 3H, H6, H5′, H6′), 7.03 (d, 2H, H2″, H6″, $J = 1,9$ Hz), 6.98 (d, 2H, H3, $J = 5.2$Hz), 6,5 (d, 1H, H4″, $J = 1.9$ Hz), 3.75 (s, 6 H, $OCH_3$). $^{13}$C NMR (67.9 MHz, δ ppm): 56.0, 56.1, 103.5, 107.4, 119.1, 122.4, 123.4, 124.6, 125.0, 125.7, 127.1, 128.2, 130.4, 134.6, 137.2, 139.6, 141.6, 145.0, 148.2, 150.2, 152.6, 161.4, 189.7. Anal. calcd. (%) $C_{26}H_{21}ClN_2O_3$: C, 70.19; H, 4.76; N, 6.30. Found: C, 70.27; H, 4.81; N, 6.47.

#### (E)-1-[3-(7-chloroquinolin-4-ylamino)phenyl]-3-(2,4,5-trimethoxyphenyl)prop-2-en-1-one (4g)

Yield: 45.74%. mp: 108–110 °C. IR (KBr pellet cm$^{-1}$): 3360 (NH), 1655 (C=O). $^1$H NMR (270 MHz, δ ppm, DMSO$d_6$): 9.30 (brs, 1H, NH), 8.50 (d, 1H, H2, $J = 5.2$Hz), 8.44 (d, 1H, H5, $J = 9.2$Hz), 8.06 (1H, Ha, $J = 15.6$ Hz), 8.00 (s, 1H, H8), 7.92–7.95 (m, 2H, H2′, H4′), 7.75 (d, 1H, Hb, $J = 15.6$ Hz), 7.58–7.68 (m, 3H, H6, H5′, H6′), 7.50 (s, 1H, H6″), 7.02 (d, 1H, H3, $J = 5.2$Hz), 6.74 (s, 1H, H3″), 3.89 (s, 3H, $OCH_3$), 3.87 (s, 3H, $OCH_3$), 3.79 (s, 3H, $OCH_3$). $^{13}$C NMR (67.9 MHz, δ ppm): 56.4, 57.0, 98.1, 102.8, 111.6, 114.8, 119.0, 122.2, 124.5, 125.0, 125.8, 126.8, 128.3, 130.4, 134.6, 139.5, 140.0, 141.4, 143.7, 148.1, 150.2, 152.6, 153.6, 155.0, 189.4. Anal. calcd. (%) $C_{27}H_{23}ClN_2O_4$: C, 68.28; H, 4.88; N, 5.90. Found: C, 68.31; H, 4.90; N, 6.11.

#### (E)-1-[3-(7-chloroquinolin-4-ylamino)phenyl]-3-(3,4,5-trimethoxyphenyl)prop-2-en-1-one (4h)

Yield: 65.32%. mp: 250–251 °C. IR (KBr pellet cm$^{-1}$): 3360 (NH), 1660 (C=O). $^1$H NMR (270 MHz, δ ppm, DMSO$d_6$): 9.33 (brs, 1H, NH), 8.52 (d, 1H, H2, $J = 5.2$Hz), 8.44 (d, 1H, H5, $J = 9.2$Hz), 8.04 (s, 1H, H8), 7.85–7.90 (m, 3H, H2′, H4′, Ha), 7.72 (d, 1H, Hb, $J = 15.6$ Hz), 7.63–7.70 (m, 1H, H6), 7.25 (s, 2H, H2″, H6″), 7.03 (d, 1H, H3, $J = 5.2$Hz), 3.85 (s, 6 H, $OCH_3$), 3.71 (s, 3H, $OCH_3$). $^{13}$C NMR (67.9 MHz, δ ppm, $CDCl_3$): 55.5, 102.9, 103.1, 106.6, 118.4, 122.1, 122.3, 124.7, 126.4, 126.5, 129.2, 130.1, 135.6, 136.6, 125.0, 139.9, 140.5, 145.6, 147.2, 152.1, 161.2, 189.9. Anal. calcd. (%) $C_{27}H_{23}ClN_2O_4$: C, 68.28; H, 4.88; N, 5.90. Found: C, 68.29; H, 4.93; N, 6.19.

#### (E)-1-[3-(7-chloroquinolin-4-ylamino)phenyl]-3-(2,4,5-trimethylphenyl)prop-2-en-1-one (4i)

Yield: 55.03%. mp: 216–217 °C. IR (KBr pellet cm$^{-1}$): 3448 (NH), 1648 (C=O), $^1$H NMR (270 MHz, δ ppm, DMSO$d_6$): 9.32 (brs, 1H, NH), 8.51 (d, 1H, H2, $J = 5.2$Hz), 8.45 (d, 1H, H5, $J = 9.2$Hz), 8.05 (s, 1H, H8), 7.92–8.01 (m, 4 H, H2′, H5′, Ha, H6″), 7.60–7.81 (m, 5 H, H6, H4′, H5′, H6′, Hb), 7.06 (s, 1H, H3″), 7.02 (d, 1H, H3, $J =$

5.2Hz), 2.37 (s, 3H, $CH_3$), 2.23 (s, 3H, $CH_3$), 2.21 (s, 3H, $CH_3$). $^{13}C$ NMR (67.9 MHz, δ ppm): 19.2, 19.4, 19.9, 102.8, 119.1, 121.8, 122.3, 124.5, 125.0, 125.7, 127.0, 128.2, 128.3, 130.4, 131.0, 132.6, 134.6, 134.8, 136.2, 139.6, 140.0, 141.5, 142.0, 148.1, 150.2, 152.6, 189.3. Anal. calcd. (%) $C_{27}H_{23}ClN_2O$: C, 75.96; H, 5.43; N, 6.56. Found: C, 76.04; H, 5.48; N, 6.74.

#### (E)-1-[3-(7-chloroquinolin-4-ylamino)phenyl]-3-(benzo[d][1,3]dioxol-6-yl) prop-2-en-1-one (4j)

Yield: 45.00%. mp: 181–183 °C. IR (KBr pellet cm−1): 3434 (NH), 1660 (C=O). $^1H$ NMR (270 MHz, δ ppm, DMSO$d_6$): 9.30 (brs, 1H, NH), 8.52 (d, 1H, H2, $J = 5.2$Hz), 8.43 (d, 1H, H5, $J = 9.2$Hz), 8.05 (s, 1H, H8), 7.92 (m, 2H, H2′, H4′), 7.80 (d, 1H, Ha, $J = 15.6$ Hz), 7.72 (s, 1H, H6″), 7.58–7.65 (m, 4H, H6, H5′, H6′, Hb), 7.32 (d, 1H, H2″, $J =$ 7.9 Hz), 6.97–7.00 (m, 2H, H3, H3″), 6.09 (s, 2H, H7"). $^{13}C$ NMR (67.9 MHz, δ ppm): 102.2, 102.7, 107.5, 109.1, 118.9, 120.5, 122.5, 124.6, 125.0, 125.7, 126.7, 127.2, 128.2, 129.7, 130.5, 134.6, 139.6, 141.4, 145.0, 148.3, 148.7, 150.1, 150.2, 152.6, 189.3. Anal. calcd. (%) $C_{25}H_{27}ClN_2O_3$: C, 70.01; H, 4.00; N, 6.53. Found: C, 69.97; H, 4.03; N, 6.70.

#### (E)-1-[3-(7-chloroquinolin-4-ylamino)phenyl]-3p-chlorophenylprop-2-en-1-one (4k)

Yield: 72.00%. mp: 204–205 °C. IR (KBr pellet $cm^{-1}$): 3426 (NH), 1650 (C=O). $^1H$ NMR (270 MHz, δ ppm, DMSO$d_6$): 9.30 (brs, 1H, NH), 8.51 (d, 1H, H2, $J = 5.2$Hz), 8.51 (d, 1H, H5, $J = 9.2$Hz), 8.43 (s, 1H, H8), 7.58–7.97 (m, 9H, H6, H2′, H4′, H5′, H6′, Ha, Hb, H2″, H6″), 7.50 (d, 2H, H3″, H5″, $J = 8.4$ Hz), 7.01 (d, 1H, H3, $J = 5.2$Hz). $^{13}C$ NMR (67.9 MHz, δ ppm): 102.8, 119.0, 122.4, 123.3, 124.7, 125.0, 125.7, 127.2, 128.2, 129.5, 130.5, 131.2, 134.1, 134.5, 135.7, 139.3, 141.5, 143.4, 148.0, 150.3, 152.6, 189. 4. Anal. calcd. (%) $C_{24}H_{16}Cl_2N_2O$: C, 68.75; H, 3.85; N, 6.68. Found: C, 68.79; H, 3.87; N, 6.91.

#### (E)-1-[4-(7-chloroquinolin-4-ylamino)phenyl]-3-p-tolylprop-2-en-1-one (5a)

Yield: 48.30%. mp: 239–241 °C. IR (KBr pellet $cm^{-1}$): 3440 (NH), 1664 (C=O). $^1H$ NMR (270 MHz, δ ppm, DMSO$d_6$): 9.50 (brs, 1H, NH), 8.62 (d, 1H, H2, $J = 5.2$Hz), 8.39 (d, 1H, H5, $J = 9.2$Hz), 8.20 (d, 2H, H3′, H5′, $J =$ 8.7 Hz), 7.97 (d, 1H, H8, $J = 2.2$Hz), 7.92 (d, 1H, Ha, $J =$ 15.6 Hz), 7.78 (d, 2H, H2″, H6″, $J = 8.2$Hz), 7.70 (d, 1H, Hb, $J = 15.6$ Hz), 7.61 (dd, 1H, H6, $J = 2.2$Hz, $J = 9.2$Hz), 7.49 (d, 2H, H2′, H6′, $J = 8.7$ Hz), 7.31 (d, 1H, H3, $J =$ 5.2Hz), 7.27 (d, 2H, H3″, H5″, $J = 8.2$Hz), 2.35 (s, 3H, $CH_3$). $^{13}C$ NMR (67.9 MHz, δ ppm): 21.7, 105.7, 119.7, 119.9, 121.5, 125.3, 126.2, 128.4, 129.4, 130.1, 131.0, 132.2, 132.7, 134.8, 141.1, 143.9, 146.3, 146.6, 150.2, 152.7, 187.7. Anal. calcd. for $C_{25}H_{19}ClN_2O$: (%) C, 75.28; H, 4.80; N, 7.02. Found: (%) C, 75.33; H, 4.80; N, 7.19.

#### (E)-1-[4-(7-chloroquinolin-4-ylamino)phenyl]-3-(2,3-dimethoxyphenyl)prop-2-en-1-one (5b)

Yield: 48.30%. mp: 194–196 °C. IR (KBr pellet $cm^{-1}$): 3426 (NH), 1660 (C=O). $^1H$ NMR (270 MHz, δ ppm, DMSO$d_6$): 9.50 (brs, 1H, NH), 8.62 (d, 1H, H2, $J = 5.2$Hz), 8.39 (d, 1H, H5, $J = 9.2$Hz), 8.19 (d, 2H, H3′, H5′ $J = 8.7$ Hz), 7.94–7.96 (m, 3H, H8, Ha, H6″), 7.60–7.64 (m, 2H, H6, Hb), 7.49 (d, 2H, H2′, H6′, $J = 8.7$ Hz), 7.31 (d, 1H, H3, $J = 5.2$Hz), 7.15 (m, 2H, H4″, H5″), 3.83 (s, 3H, $OCH_3$), 3.80 (s, 3H, $OCH_3$). $^{13}C$ NMR (67.9 MHz, δ ppm): 56.4, 61.6, 105.8, 115.4, 119.7, 119.8, 119.9, 123.4, 124.9, 125.3, 126.2, 128.3, 128.9, 131.0, 132.1, 134.9, 137.8, 146.4, 146.5, 148.8, 150.2, 152.7, 153.3, 187.8. Anal. calcd. for $C_{26}H_{21}ClN_2O_3$: (%) C, 70.19; H, 4.76; N, 6.30. Found: (%) C, 70.22; H, 4.77; N, 6.53.

#### (E)-1-[4-(7-Chloroquinolin-4-ylamino)phenyl]-3-(2,4-dimethoxyphenyl)prop-2-en-1-one (5c)

Yield: 55.30%. mp: 215–217 °C. IR (KBr pellet $cm^{-1}$): 3434 (NH), 1660 (C=O). $^1H$ NMR (270 MHz, δ ppm, DMSO$d_6$): 9.46 (brs, 1H, NH), 8.61 (d, 1H, H2, $J = 5.2$Hz), 8.40 (d, 1H, H5, $J = 9.2$Hz), 8.15 (d, 2H, H3′, H5′, $J = 8.7$ Hz), 7.96–8.02 (m, 2H, H8, Ha), 7.91 (d, 1H, H6″, $J = 8.4$ Hz), 7.78 (d, 1H, Hb, $J = 15.6$ Hz), 7.62 (dd, 1H, H6, $J = 9.2$Hz, $J = 1.9$ Hz), 7.48 (d, 2H, H2′, H6′, $J = 8.7$ Hz), 7.30 (d, 1H, H3, $J =$ 5.2Hz), 6.61 (m, 2H, H3″, H5″), 3.90 (s, 3H, $OCH_3$), 3.84 (s, 3H, $OCH_3$). $^{13}C$ NMR (67.9 MHz, δ ppm): 56.1, 56.4, 99.0, 105.6, 107.0, 116.8, 119.8, 120.0, 125.3, 126.0, 128.4, 130.7, 132.8, 134.8, 138.7, 146.0, 146.8, 150.3, 152,6, 160.5, 163.4, 188.0. Anal. calcd. for $C_{26}H_{21}ClN_2O_3$: (%) C, 70.19; H, 4.76; N, 6.30. Found: (%) C, 70.23; H, 4.75; N, 6.47.

#### (E)-1-[4-(7-chloroquinolin-4-ylamino)phenyl]-3-(2,5-dimethoxyphenyl)prop-2-en-1-one (5d)

Yield: 50.30%. mp: 178–180 °C. IR (KBr pellet $cm^{-1}$): 3448 (NH), 1657 (C=O). $^1H$ NMR (270 MHz, δ ppm, DMSO$d_6$): 9.52 (brs, 1H, NH), 8.62 (d, 1H, H2, $J = 5.2$Hz), 8.40 (d, 1H, H5, $J = 9.2$ Hz), 8.20 (d, 2H, H3′, H5′, $J =$ 8.7 Hz), 7.90–8.07 (m, H8, Ha, H6″), 7.64 (dd, 1H, H6, $J =$ 9.2 Hz, $J = 1.9$ Hz), 7.56 (d, Hb, $J = 15.6$ Hz), 7.49 (d, 2H, H2′, H6′, $J = 8.7$ Hz), 7.32 (d, 1H, H3, $J = 5.2$Hz), 7.04 (m, 2H, H3″, H4″), 3.84 (s, 3H, $OCH_3$), 3.80 (s, 3H, $OCH_3$). $^{13}C$ NMR (67.9 MHz, δ ppm): 56.2, 56.7, 105.7, 113.0, 113.6, 118.5, 119.7, 119.9, 122.5, 124.2, 125.6, 126.1, 128.4, 131.0, 132.2, 134.7, 138.1, 146.3, 146.6, 150.2, 152.6, 153.2, 153.8, 187.8. Anal. calcd. (%) $C_{26}H_{21}ClN_2O_3$: C, 70.19; H, 4.76; N, 6.30. Found: C, 70.17; H, 4.76; N, 6.49.

### (E)-1-[4-(7-chloroquinolin-4-ylamino)phenyl]-3-(3,4-dimethoxyphenyl)prop-2-en-1-one (5e)

Yield: 45.80%. mp: 204–205 °C. IR (KBr pellet $cm^{-1}$): 3424 (NH), 1645 (C=O). $^1$H NMR (270 MHz, δ ppm, DMSO$d_6$): 9.52 (brs, 1H, NH), 8.62 (d, 1H, H2, $J = 5.2$Hz), 8.41 (d, 1H, H5, $J = 9.2$ Hz), 8.21 (d, 2H, H3′, H6′, $J =$ 8.7 Hz), 7.96 (s, 1H, H8), 7.87 (d, 1H, Ha, $J = 15.6$ Hz), 7.68 (d, 1H, Hb, $J = 15.6$ Hz), 7.64 (dd, 1H, H6, $J = 9.2$Hz, $J = 1.9$ Hz), 7.54 (s, 1H, H2″), 7.49 (d, 2H, H2′, H6′, $J =$ 8.7 Hz), 7.38 (d, 1H, H6″, $J = 8.7$ Hz), 7.31 (d, 1H, H3, $J =$ 5.2Hz), 7.02 (d, 1H, H5″, $J = 8.7$ Hz), 3.86 (s, 3H, $OCH_3$), 3.81 (s, 3H, $OCH_3$). $^{13}$C NMR (67.9 MHz, δ ppm): 56.2, 56.3, 105.3, 111.0, 112.2, 119.8, 121.0, 124.4, 125.3, 126.1, 128.2, 128.3, 130.9, 132.5, 134.7, 144.3, 146.7, 149.6, 150.2, 151.7, 152.2, 152.4, 187.9. Anal. calcd. for $C_{26}H_{21}ClN_2O_3$: (%) C, 70.19; H, 4.76; N, 6.30. Found: (%) C, 70.27; H, 4.83; N, 6.42.

### (E)-1-[4-(7-chloroquinolin-4-ylamino)phenyl]-3-(3,5-dimethoxyphenyl)prop-2-en-1-one (5f)

Yield: 46.50%. mp: 129–131 °C. IR (KBr pellet $cm^{-1}$): 3424 (NH), 1649 (C=O). $^1$H NMR (270 MHz, δ ppm, DMSO$d_6$): 9.51 (brs, 1H, NH), 8.63 (d, 1H, H2, $J = 5.2$Hz), 8.40 (d, 1H, H5, $J = 9.2$Hz), 8.23 (d, 2H, H3′, H5′, $J =$ 8.7 Hz), 7.98 (d, 1H, H8, $J = 1.9$ Hz), 7.97 (d, 1H, Ha, $J =$ 15.6 Hz), 7.61–7.68 (m, 2H, H6, Hb), 7.49 (d, 2H, H2′, H6′, $J = 8.7$ Hz), 7.32 (d, 1H, H3, $J = 5.2$Hz), 7.07 (d, 2H, H2″, H6″, $J = 1.9$ Hz), 6.58 (s, 1H, H4″), 3.81 (s, 6H, $OCH_3$). $^{13}$C NMR (67.9 MHz, δ ppm): 56.0, 103.4, 105.9, 107.3, 119.7, 120.0, 123.2, 125.3, 126.1, 128.4, 131.1, 132.2, 134.9, 137.4, 143.8, 146.5, 146.6, 150.3, 152.6, 161.4, 187.8. Anal. calcd. for $C_{26}H_{21}ClN_2O_3$: (%) C, 70.19; H, 4.76; N, 6.30. Found: (%) C, 70.19; H, 4.78; N, 6.43.

### (E)-1-[4-(7-chloroquinolin-4-ylamino)phenyl]-3-(2,4,5-trimethoxyphenyl)prop-2-en-1-one (5g)

Yield: 79.50%. mp: 120–121 °C. IR (KBr pellet $cm^{-1}$): 3436 (NH), 1658 (C=O). $^1$H NMR (270 MHz, δ ppm, DMSO$d_6$): 9.49 (brs, 1H, NH), 8.62 (d, 1H, H2, $J = 5.2$Hz), 8.41 (d, 1H, H5, $J = 9.2$Hz), 8.20 (d, 2H, H3′, H5′, $J =$ 8.7 Hz), 8.06 (d, 1H, Ha, $J = 15.6$ Hz), 7.97 (d, 1H, H8, $J =$ 1.9 Hz), 7.80 (d, 1H, Hb, $J = 15.6$ Hz), 7.63 (d, 1H, H6, $J = 9.2$Hz), 7.48–7.53 (m, 3H, H2′, H6′, H6″), 7.31 (d, 1H, H3, $J = 5.2$Hz), 6.75 (s, 1H, H3″), 3.90 (s, 3H, $OCH_3$), 3.87 (s, 3H, $OCH_3$), 3.83 (s, 3H, $OCH_3$). $^{13}$C NMR (67.9 MHz, δ ppm): 56.4, 56.9, 57.0, 98.2, 105.4, 111.3, 114.9, 119.1, 119.9, 125.3, 126.0, 128.2, 130.8, 132.7, 134.9,138.3, 143.7, 146.0, 146.7, 150.2, 152.6, 153.3, 154.8, 187.7. Anal. calcd. (%) $C_{27}H_{23}ClN_2O_4$: C, 68.28; H, 4.88; N, 5.90. Found: C, 68.29; H, 4.92; N, 6.13.

### (E)-1-(4-(7-chloroquinolin-4-ylamino)phenyl)-3-(3,4,5-trimethoxyphenyl)prop-2-en-1-one (5h)

Yield: 52.69 %. mp: 116–118 °C. IR (KBr pellet $cm^{-1}$): 3424 (NH), 1668. $^1$H NMR (270 MHz, δ ppm, DMSO*d*6): 9.50 (brs, 1H, NH), 8.62 (d, 1H, H2, $J = 5.2$Hz), 8.40 (d, 1H, H5, $J = 9.2$Hz), 8.23 (d, 2H, H3′, H5′, $J = 8.7$ Hz), 7.96 (s, 1H, H8), 3.71 (s, 3H, $OCH_3$), 7.92 (d, 1H, Ha, $J = 15.6$ Hz), 7.68 (d, 1H, Hb, $J = 15.6$ Hz), 7.62 (dd, 1H, H6, $J = 9.2$Hz), 7.50 (d, 2H, H2′, H6′ $J = 8.7$ Hz), 7.31 (d, 1H, H3, $J =$ 5.2Hz), 7.23 (s, 2H, H2″, H6″), 3.87 (s, 6H, $OCH_3$), 3.72 (s, 3H, $OCH_3$). $^{13}$C NMR (67.9 MHz, δ ppm): 56.7, 60.7, 105.7, 107.0, 119.7, 119.9, 121.7, 125.3, 126.1, 128.3, 131.0, 131.1, 132.2, 134.8, 140.2, 144.3, 146.4, 146.7 150.2, 152.5, 153.7, 187.7. Anal. calcd. (%) $C_{27}H_{23}ClN_2O_4$: C, 68.28; H, 4.88; N, 5.90. Found: C, 68.25; H, 4.90; N, 6.07.

### (E)-1-[4-(7-chloroquinolin-4-ylamino)phenyl]-3-(2,4,5-trimethylphenyl)prop-2-en-1-one (5i)

Yield: 52.50%. mp: 228–230 °C. IR (KBr pellet cm−1): 3420 (NH), 1645 (C=O). $^1$H NMR (270 MHz, δ ppm, DMSO$d_6$): 9.51 (brs, 1H, NH), 8.62 (d, 1H, H2, $J =$ 5.21Hz), 8.40 (d, 1H, H5, $J = 9.15$ Hz), 8.20 (d, 2H, H3′, H5′, $J = 8.67$ Hz), 7.92–7.97 (m, 2H, H8, Ha), 7.79–7.85 (m, 2H, Hb, H6″), 7.63 (d, 2H, H6, $J = 9.15$ Hz), 7.50 (d, 2H, H2′, H6′, $J = 8.67$ Hz), 2.22 (s, 3H, $CH_3$), 7.31 (d, 1H, H3, $J = 5.21$Hz), 7.05 (s, 1H, H3″), 2.49 (s, 3H, $CH_3$), 2.37 (s, 3H, $CH_3$) 2.33 (s, 3H, $CH_3$). $^{13}$C NMR (67.9 MHz, δ ppm): 19.3, 19.4, 19.9, 105.7, 119.8, 119.9, 121.8, 125.2, 126.1, 128.2, 128.3, 128.4, 131.0, 131.2, 132.2, 132.5, 134.8, 135.9, 139.7, 140.8, 146.3, 146.6, 150.1, 152.8, 187.7. Anal. calcd. (%) $C_{27}H_{23}ClN_2O$: C, 75.96; H, 5.43; N, 6.56. Found: C, 75.93; H, 5.49; N, 6.67.

### (E)-1-[4-(7-cloroquinolin-4-ylamino)phenyl]-3-(benzo[d][1,3]dioxol-6-yl)prop-2-en-1-one (5j)

Yield: 51.60%. mp: 190–191 °C. IR (KBr pellet $cm^{-1}$): 3470 (NH), 1659 (C=O). $^1$H NMR (270 MHz, δ ppm, DMSO$d_6$): 9.51 (brs, 1H, NH), 8.63 (d, 1H, H2, $J =$ 5.2Hz), 8.40 (d, 1H, H5, $J = 9.2$Hz), 8.21 (d, 2H, H3′, H5′, $J = 8.7$ Hz), 7.98 (d, 1H, H8, $J = 1.9$ Hz), 7.86 (d, 1H, Ha, $J = 15.6$ Hz), 7.63–7.70 (m, 3H, H6, Hb, H2″), 7.49 (d, 2H, H2′, H6′, $J = 8.7$ Hz), 7.30–7.35 (m, 2H, H5″, H6″), 7.00 (d, 1H, H3, $J = 9.2$Hz), 6.12 (s, 2H, H7''). $^{13}$C NMR (67.9 MHz, δ ppm): 102.2, 105.6, 107.5, 109.1, 119.8, 120.0, 121.0, 125.3, 126.1, 126.3, 128.3, 129.9, 131.0, 132.3, 134.8, 143.8, 146.4, 146.7, 148.7, 150.0, 150.2, 152.6, 187.6. Anal. calcd. (%) $C_{25}H_{27}ClN_2O_3$: C, 70.01; H, 4.00; N, 6.53. Found: C, 70.06; H, 4.12; N, 6.73.

#### (E)-1-[4-(7-chloroquinolin-4-ylamino)phenyl]-3–p-chlorophenylprop-2-en-1-one (5k)

Yield: 49.50%. mp: 120–121 °C. IR (KBr pellet cm−1): 3424 (NH), 1544 (C=O). $^1$H NMR (270 MHz, δ ppm, DMSO$d_6$): 9.50 (brs, 1H, NH), 8.62 (d, 1H, H2, $J$ = 5.2Hz), 8.39 (d, 1H, H5, $J$ = 9.2Hz), 8.20 (d, 2H, H3′, H5′, $J$ = 8.7 Hz), 7.90–8.01 (m, 4 H, H8, Ha, H2″, H6″), 7.70 (d, 1H, Hb, $J$ = 15.6 Hz), 7.62 (dd, 1H, H6, $J$ = 9.2, $J$ = 1.9 Hz), 7.47–7.53 (m, 4 H, H2′, H6′, H3″, H5″), 7.30 (d, 1H, H3, $J$ = 9.2Hz). $^{13}$C NMR (67.9 MHz, δ ppm): 105.7, 119.6, 119.9, 121.7, 125.3, 126.2, 128.3, 129.7, 131.1, 131.2, 132.0, 133.8, 134.2, 134.4, 134.8, 135.5, 142.0, 142.3, 146.5, 152.5, 187.5. Anal. calcd. (%) $C_{24}H_{16}Cl_2N_2O$: C, 68.75; H, 3.85; N, 6.68. Found. C, 68.91; H, 3.86; N, 6.83.

### General procedure for the synthesis of the 7-chloro-N-{3 or 4-[4,5-dihydro-5-(phenyl-substituted)-1H-pyrazol-3-yl]phenyl}quinoline-4-amine derivatives (6, 7)

In a round bottomed flask with a condenser, magnetic stirring and heating, 100 mg of the respective quinoline-chalcone hybrids derivative, hydrazine monohydrate 1 mL, glacial acetic acid catalytic amounts, and 5 mL of dry ethanol were placed under the conditions of reflux for 24 h, obtaining a solid that was washed with water, ethyl ether, dried under vacuum, and recrystallized from ethanol-water (1/1).

#### 7-Chloro-N-{3-[4,5-dihydro-5-(3,4-dimethoxyphenyl)-1H-pyrazol-3-yl]phenyl} quinolin-4–amine (6e)

Yield: 79.50%. mp: 180–181 °C. IR (KBr pellet cm$^{-1}$): 3268 (NH). $^1$H NMR (270 MHz, δ ppm, DMSO$d_6$): 9.15 (brs, 1H, NH), 8.47 (d, 1H, H2, $J$ = 5.2Hz), 8.42 (d, 1H, H5, $J$ = 9.2Hz), 7.90 (d, 1H, H8, $J$ = 1.9 Hz), 7.64 (s, 1H, H2′), 7.57 (dd, 1H, H6, $J$ = 9. 2Hz, $J$ = 1.9 Hz), 7.30–7.42 (m, 3H, H4′, H5′, H6′), 6.89–6.94 (m, 4 H, H3, H2″, H5″, H6″), 4.79 (td, 1H, Hb, $J$ = 10.9 Hz, $J$ = 2.8 Hz), 3.74 ($OCH_3$), 3.72 ($OCH_3$), 3.32–3.45 (m, 1H, Ha), 2.85 (dd, 1H, Ha, $J$ = 16.2HZ, $J$ = 10.9 Hz). $^{13}$C NMR (67.9 MHz, δ ppm): 41.0, 56.1, 56.3, 64.2, 102.6, 111.3, 112.6, 119.2, 119.6, 121.8, 122.6, 125.0, 125.5, 128.3, 129.7, 130.1, 134.5, 135.3, 135.9, 141.0, 148.5, 148.7, 148.9, 149.4, 150.2, 152.5. Anal. calcd. (%) $C_{26}H_{23}ClN_4O_2$: C, 68.04; H, 5.05; N, 12.21. Found: C, 67.93; H, 5.08; N, 12.50.

#### 7-Chloro-N-{3-[4,5-dihydro-5-(3,5-dimethoxyphenyl)-1H-pyrazol-3-yl]phenyl} quinolin-4–amine (6f)

Yield: 78.2%. mp: 119–121 °C. IR (KBr pellet cm$^{-1}$): 3235 (NH). $^1$H NMR (270 MHz, δ ppm, DMSO$d_6$): 9.16 (brs, 1H, NH), 8.47 (d, 1H, H2, $J$ = 5.2Hz), 8.43 (d, 1H, H5, $J$ = 9.2Hz), 7.90 (d, 1H, H8, $J$ = 1.9 Hz), 7.63 (s, 1H, H2′), 7.57 (dd, 1H, H6, $J$ = 9.2Hz, $J$ = 1.9 Hz), 7.30–7.45 (m, 3H, H4′, H5′, H6′), 6.96 (d, 1H, H3, $J$ = 5.2Hz), 6.55 (d, 2H, H2″, H6″, $J$ = 1.9 Hz), 6.39 (t, 1H, H4″, $J$ = 1.9 Hz), 4.79 (td, 1H, Hb, $J$ = 10.9 Hz, $J$ = 2.8 Hz), 3.72 (s, 6 H, $OCH_3$), 3.35 (m, 1H, Ha), 2.84 (dd, 1H, Ha, $J$ = 16.2Hz, $J$ = 10.9 Hz). $^{13}$C NMR (67.9 MHz, δ ppm): 41.0, 55.7, 64.3, 99.5, 102.7, 105.2, 119.0, 119.7, 121.7, 122.6, 125.0, 125.5, 128.2, 130.1, 134.5, 135.2, 141.0, 146.0, 148.5, 148.8, 150.2, 152.5, 161.1. Anal. calcd. (%) $C_{26}H_{23}ClN_4O_2$: C, 68.04; H, 5.05; N, 12.21. Found: C, 68.05; H, 5.07; N, 12.47.

#### 7-Chloro-N-{3-[4,5-dihydro-5-(2,4,5-trimethoxyphenyl)-1H-pyrazol-3-yl]phenyl}quinolin-4–amine (6 g)

Yield: 71.02%. mp: 116–118 °C. IR (KBr pellet cm$^{-1}$): 3216 (NH). $^1$H NMR (270 MHz, δ ppm, DMSO$d_6$): 9.14 (brs, 1H, NH), 8.47 (d, 1H, H2, $J$ = 5.2Hz), 8.42 (d, 1H, H5, $J$ = 9.2Hz), 7.89 (d, 1H, H8, $J$ = 1.9 Hz), 7.62 (s, 1H, H2′), 7.57 (dd, 1H, H6, $J$ = 9.2Hz, $J$ = 1.9 Hz), 7.29–7.46 (m, 4 H, H4′, H5′, H6′), 6.99 (s, 1H, H3″), 6.96 (d, 1H, H3, $J$ = 5.2Hz), 6.69 (s, 1H, H6″), 4.99 (td, 1H, Hb, $J$ = 10,9 Hz, $J$ = 2.79 Hz), 3.79 (s, 3H, $OCH_3$), 3.77 (s, 3H, $OCH_3$), 3.67 (s, 3H, $OCH_3$), 3.38 (m, 1H, Ha), 2.69 (dd, 1H, Ha, $J$ = 16.2Hz, $J$ = 10.9 Hz). $^{13}$C NMR (67.9 MHz, δ ppm): 40.0, 56.6, 57.0, 57.2, 99.5, 102.6, 112.6, 119.0, 119.7, 121.7, 122.5, 122.7, 125.0, 125.5, 128.1, 130.0, 134.5, 135.3, 141.0, 143.3, 148.6, 149.0, 149.4, 150.1, 151.6, 152.4. Anal. calcd. (%) $C_{27}H_{25}ClN_4O_3$: C, 66.32; H, 5.15; N, 11.46. Found: C, 66.37; H, 5.16; N, 11.73.

#### 7-Chloro-N-{3-[4,5-dihydro-5-(3,4,5-trimethoxyphenyl)-1H-pyrazol-3-yl]phenyl}quinolin-4–amine (6 h)

Yield: 73.25%. mp: 219–221 °C. IR (KBr pellet cm$^{-1}$): 3216 (NH). $^1$H NMR (270 MHz, δ ppm, DMSO$d_6$): 9.12 (brs, 1H, NH), 8.43 (d, 1H, H2, $J$ = 5.2Hz), 8.40 (d, 1H, H5, $J$ = 9.1Hz), 7.89 (d, 1H, H8, $J$ = 1.9 Hz), 7.61 (s, 1H, H2′), 7.59 (s, 2H, H2″, 6″), 7.55 (dd, 1H, H6, $J$ = 9.1Hz, $J$ = 1.9 Hz), 7.29–7.46 (m, 4 H, H4′, H5′, H6′), 6.92 (d, 1H, H3, $J$ = 5.2Hz), 4.93 (td, 1H, Hb, $J$ = 10,9 Hz, $J$ = 2.8 Hz), 3.78 (s, 6H, $OCH_3$), 3.69 (s, 3H, $OCH_3$), 3.32 (m, 1H, Ha), 2.75 (dd, 1H, Ha, $J$ = 16.1Hz, $J$ = 10.9 Hz). $^{13}$C NMR (67.9 MHz, δ ppm): 40.2, 56.9, 57.3, 57.7, 57.8, 98.9, 101.0, 111.4, 120.3, 120.7, 121.5, 122.3, 122.7, 125.4, 125.7, 128.0, 130.2, 133.4, 135.1, 140.0, 143.7, 147.9, 149.4, 149.7, 150.2, 151.0, 152.3. Anal. calcd. (%) $C_{27}H_{25}ClN_4O_3$: C, 66.32; H, 5.15; N, 11.46. Found: C, 66.40: H, 5.21, N, 11.63.

#### 7-Chloro-N-{3-[4,5-dihydro-5-(2,4,5-trimethylphenyl)-1H-pyrazol-3-yl]phenyl} quinolin-4–amine (6i)

Yield: 67.20%. mp: 197–199 °C. IR (KBr pellet cm$^{-1}$): 3245 (NH). $^1$H NMR (270 MHz, δ ppm, DMSO$d_6$): 9.14

(brs, 1H, NH), 8.47 (d, 1H, H2, $J = 5.2$Hz), 8.42 (d, 1H, H5, $J = 9.2$Hz), 7.89 (d, 1H, H8, $J = 1.9$ Hz), 7.63 (s, 1H, H2′), 2.14 ($2CH_3$), 2.32 ($CH_3$), 7.57 (dd, 1H, H6, $J =$ 9.2Hz, $J = 1.9$ Hz), 7.51 (d, 1H, H4′, $J = 2.2$Hz), 7.29–7.44 (m, 2H, H5′, H6′), 7.18 (s, 1H, H6″), 6.95 (d, 1H, H3, $J =$ 5.2Hz), 6.92 (s, 1H, H3″), 4.94 (td, 1H, Hb, $J = 10.9$ Hz, $J = 2.8$ Hz), 3.47 (dd, 1H, Ha, $J = 16.2$Hz, $J = 10.9$ Hz), 2.67 (dd, 1H, Ha, $J = 16.2$Hz, $J = 10.9$ Hz). $^{13}$C NMR (67.9 MHz, δ ppm): 18.9, 19.3, 19.6, 40.0, 61.0, 102.5, 118.9, 119.8, 121.8, 122.6, 125.0, 125.6, 127.5, 128.0, 130.1, 132.1, 132.6, 133.8, 134.6, 134.9, 135.4, 138.6, 140.9, 148.2, 148.7, 149.8, 152.2. Anal. calcd. (%) $C_{27}H_{25}ClN_4$: C, 73.54; H, 5.71; N, 12.71. Found: C, 73.59; H, 5.72; N, 12.90.

### 7-Chloro-N-{3-[4,5-dihydro-5-(4-Chlorophenyl)-1H-pyrazol-3-yl]phenyl}-quinolin-4–amine (6k)

Yield: 71.80%. mp: 118–120 °C. IR (KBr pellet $cm^{-1}$): 3325 (NH). $^1$H NMR (270 MHz, δ ppm, DMSO$d_6$): 9.15 (s, 1H, NH), 8.47 (d, 1H, H2, $J = 5.2$Hz), 8.42 (d, 1H, H5, $J = 9.2$Hz), 7.89 (d, 1H, H8, $J = 1.9$ Hz), 7.69 (d, 1H, H2′, $J = 2.9$ Hz), 7.63 (s, 1H, NH), 7.57 (dd, 1H, H6, $J =$ 9.2Hz, $J = 1.9$ Hz), 7.30–7.45 (m, 7 H, H4′, H5′, H6′, H2″, H6″, H3″, H5″), 6.96 (d, 1H, H3, $J = 5.1$Hz), 4.86 (td, 1H, Hb, $J = 10.9$ Hz, $J = 2.8$ Hz), 3.42 (dd, 1H, Ha, $J = 16.2$Hz, $J = 10.9$ Hz), 2.83 (dd, 1H, Ha, $J = 16.2$Hz, $J = 10.9$ Hz). $^{13}$C NMR (67.9 MHz, δ ppm): 40.4, 63.5, 102.3, 118.9, 119.8, 121.9, 122.6, 125.0, 125.6, 127.9, 128.9, 129.0, 129.8, 130.1, 134.7, 135.0, 141.0, 142.6, 148.8, 149.8, 152.1. Anal. calcd. (%) $C_{24}H_{18}Cl_2N_4$: C, 66.52; H, 4.19; N, 12.93. Found: C, 66.47; H, 4.17; N, 13.11.

### 7-Chloro-N-{4-[4,5-dihydro-5-(2,4-dimethoxyphenyl)-1H-pyrazol-3-yl]phenyl} quinoline-4–amine (7c)

Yield: 75.02%. mp: 160–162 °C. IR (KBr pellet $cm^{-1}$): 3345 (NH). $^1$H NMR (270 MHz, δ ppm, DMSO$d_6$): 9.11 (brs, 1H, NH), 8.47 (d, 1H, H2, $J = 5.2$Hz), 8.41 (d, 1H, H5, $J = 9.2$Hz), 7.90 (s, 1H, H8), 7.55–7.68 (m, 3H, H3, H3′, H5′), 7.23–7.36 (m, 3H, H6, H2′, H6′), 6.94 (d, 1H, H3, $J = 5.2$Hz), 6.57 (d, 1H, H6″, $J = 2.2$Hz), 6.50 (dd, 1H, H5″, $J = 8.4$, $J = 2.2$Hz), 6.32 (brs, 1H, NH), 5.00 (t, 1H, Hb, $J = 10.9$ Hz), 3.81 (s, 3H, $OCH_3$), 3.74 (s, 3H, $OCH_3$), 3.35 (m, 1H, Ha), 2.70 (dd, 1H, Ha, $J = 16.2$Hz, $J = 10.9$ Hz). $^{13}$C NMR (67.9 MHz, δ ppm): 39.7, 55.7, 56.1, 58.1, 99.0, 102.6, 118.9, 122.5, 122.6, 125.0, 125.5, 126.3, 126.9, 127.9, 134.7, 136.2, 132.8, 139.8, 142.5, 150.1, 152.4. Anal. calcd. (%) $C_{26}H_{23}ClN_4O_2$: C, 68.04; H, 5.05; N, 12.21. Found: C, 68.22; H, 5.09; N, 12.37.

### 7-Chloro-N-{4-[4,5-dihydro-5-(2,5-dimethoxyphenyl)-1H-pyrazol-3-yl]phenyl} quinolin-4–amine (7d)

Yield: 74.30%. mp: 192–193 °C. IR (KBr pellet $cm^{-1}$): 3280 (NH). $^1$H NMR (270 MHz, δ ppm, DMSO$d_6$): 9.19 (brs, 1H, NH), 8.48 (d, 1H, H2, $J = 5.2$Hz), 8.42 (d, 1H, H5, $J =$ 9.2Hz), 7.90 (s, 1H, H8), 7.65 (d, 2H, H3′, H5′, $J = 8.7$ Hz), 7.57 (d, 1H, H6, $J = 9.2$Hz), 7.35 (d, 2H, H2′, H6′, $J =$ 8.7 Hz), 6.91–7.02 (m, 3H, H3, H3″, H6″), 6.79 (dd, 1H, H4″, $J = 8.4$ Hz, $J = 2.2$Hz), 5.00 (t, 1H, Hb, $J = 10.9$ Hz), 3.78 (s, 3H, $OCH_3$), 3.69 (s, 3H, $OCH_3$), 3.37 (m, 1H, Ha), 2.72 (dd, 1H, Ha, $J = 16.2$Hz, $J = 10.9$ Hz). $^{13}$C NMR (67.9 MHz, δ ppm): 40.0, 55.9, 56.5, 58.4, 103.0, 112.5, 112.7, 113.4, 119.1, 122.5, 125.1, 125.6, 127.1, 128.0, 129.5, 132.6, 134.6, 140.7, 148.3, 149.0, 149.9, 151.3, 152.3, 153.8. Anal. calcd. (%) $C_{26}H_{23}ClN_4O_2$: C, 68.04; H, 5.05; N, 12.21. Found: C, 67.97; H, 5.06; N, 12.43.

### 7-Chloro-N-{4-[4,5-dihydro-5-(3,4-dimethoxyphenyl)-1H-pyrazol-3-yl]phenyl} quinolin-4–amine (7e)

Yield: 74.08%. mp: 106–108 °C. IR (KBr pellet $cm^{-1}$): 3376 (NH). $^1$H NMR (270 MHz, δ ppm, DMSO$d_6$): 9.19 (brs, 1H, NH), 8.48 (d, 1H, H2, $J = 5.2$Hz), 8.42 (d, 1H, H5, $J =$ 9.2Hz), 7.90 (d, 1H, H8, $J = 1.9$ Hz), 7.66 (d, 2H, H3′, H5′, $J = 8.7$ Hz), 7.58 (dd, 1H, H6, $J = 9.2$Hz, $J = 1.9$ Hz), 7.46 (brs, 1H, NH), 7.37 (d, 2H, H2′, H6′, $J = 8.7$ Hz), 6.90–7.00 (m, 4 H, H3, H2″, H5″, H6″), 4.78 (t, 1H, Hb, $J = 10.9$ Hz), 3.75 (s, 3H, $OCH_3$), 3.73 (s, 3H, $OCH_3$), 3.41 (m, 1H, Ha), 2.84 (dd, 1H, Ha, $J = 16.2$Hz, $J = 10.9$ Hz). $^{13}$C NMR (67.9 MHz, δ ppm): 41.2, 56.1, 56.2, 64.1, 103.0, 111.1, 112.4, 119.1, 119.3, 122.5, 125.1, 125.6, 127.1, 128.0, 128.2, 129.6, 134.6, 136.1, 140.8, 148.2, 148.7, 149.1, 149.4, 150.1, 152.4. Anal. calcd. (%) $C_{26}H_{23}ClN_4O_2$: C, 68.04; H, 5.05; N, 12.21. Found: C, 68.07; H, 5.13; N, 12.39.

### 7-Chloro-N-{4-[4,5-dihydro-5-(2,4,5-trimethoxyphenyl)-1H-pyrazol-3-yl]phenyl} quinolin-4–amine (7 g)

Yield: 76.15%. mp: 164–165 °C. IR (KBr pellet $cm^{-1}$): 3380 (NH). $^1$H NMR (270 MHz, δ ppm, DMSO$d_6$): 9.18 (brs, 1H, NH), 8.48 (d, 1H, H2, $J = 5.2$Hz), 8.42 (d, 1H, H5, $J = 9.2$Hz), 7.90 (d, 1H, H8, $J = 1.9$ Hz), 7.65 (d, 2H, H3′, H5′, $J = 8.7$ Hz), 7.57 (dd, 1H, H6, $J = 9.2$Hz, $J =$ 1.9 Hz), 7.35 (d, 2H, H2′, H6′, $J = 8.7$ Hz), 6.99–7.01 (m, 2H, H3, H6″), 6.70 (s, 1H, H3″), 4.98 (t, 1H, Hb, $J =$ 10.9 Hz), 3.80 (s, 3H, $OCH_3$), 3.78 (s, 3H, $OCH_3$), 3.67 (s, 3H, $OCH_3$), 3.35 (m, 1H, Ha), 2.70 (dd, 1H, Ha, $J =$ 16.2Hz, $J = 10.9$ Hz). $^{13}$C NMR (67.9 MHz, δ ppm): 40.5, 56.6, 56.8, 57.2, 105.3, 119.8, 120.4, 122.9, 125.2, 125.3, 125.8, 127.1, 128.1, 128.8, 129.1, 130.3, 131.4, 134.9, 134.9, 143.2, 150.0, 152.2. Anal. calcd. (%)

$C_{27}H_{25}ClN_4O_3$: C, 66.32; H, 5.15; N, 11.46. Found: C, 66.29: H, 5.17, N, 11.70.

### 7-Chloro-N-{4-[4,5-dihydro-5-(3,4,5-trimethoxyphenyl)-1H-pyrazol-3-yl]phenyl} quinolin-4–amine (7 h)

Yield: 53.08%. mp: 173–175 °C. IR (KBr pellet $cm^{-1}$): 3425 (NH), 1673. $^1$H NMR (270 MHz, δ ppm, DMSO*d*6): 9.51 (brs, 1H, NH), 8.61 (d, 1H, H2, $J = 5.2$Hz), 8.40 (d, 1H, H5, $J = 9.2$Hz), 8.37 (d, 2H, H3′, H5′, $J = 8.7$ Hz), 7.97 (s, 1H, H8), 7.57 (dd, 1H, H6, $J = 9.2$Hz), 7.49 (d, 2H, H2′, H6′, $J = 8.7$ Hz), 7.23 (d, 1H, H3, $J = 5.2$Hz), 7.61 (s, 2H, H2″, H6″), 3.81 (s, 6 H, $OCH_3$), 3.75 (s, 3H, $OCH_3$), 3.35 (m, 1H, Ha), 2.72 (dd, 1H, Ha, $J = 16.2$Hz, $J = 10.8$ Hz). $^{13}$C NMR (67.9 MHz, δ ppm): 56.5, 59.7, 104.8, 106.9, 119.5, 119.9, 121.9, 124.3, 126.3, 128.7, 129.8, 131.3, 133.4, 134.9, 141.1, 143.9, 146.8, 147.9 151.2, 152.4, 154.7. Anal. calcd. (%) $C_{27}H_{25}ClN_4O_3$: C, 66.32; H, 5.15; N, 11.46. Found: C, 66.37: H, 5.23, N, 11.81.

### 7-Chloro-N-{4-[4,5-dihydro-5-(3,4,5-trimethylphenyl)-1H-pyrazol-3-yl]phenyl} quinolin-4–amine (7i)

Yield: 72.08%. mp: 197–199 °C. IR (KBr pellet $cm^{-1}$): 3289 (NH). $^1$H NMR (270 MHz, δ ppm, DMSO$d_6$): 9.18 (brs, 1H, NH), 8.48 (d, 1H, H2, $J = 5.2$Hz), 8.42 (d, 1H, H5, $J = 9.2$Hz), 7.89 (d, 1H, H8, $J = 1.9$ Hz), 7.65 (d, 2H, H3′, H5′, $J = 8.7$ Hz), 2.15 (s, 6H, $CH_3$), 7.57 (dd, 1H, H6, $J = 9.2$Hz, $J = 1.9$ Hz), 7.36 (d, 2H, H2′, H6′, $J =$ 8.7 Hz), 7.19 (s, 1H, H6″), 7.00 (d, 1H, H3, $J = 5.2$Hz), 6.92 (s, 1H, H3″), 4.93 (t, 1H, Hb, $J = 10.9$ Hz), 3.45 (dd, 1H, Ha, $J = 16.2$Hz, $J = 10.9$ Hz), 2.67 (dd, 1H, Ha, $J =$ 16.2Hz, $J = 10.9$ Hz), 2.25 (s, 3H, $CH_3$), 2.14 (s, 6H, $CH_3$). $^{13}$C NMR (67.9 MHz, δ ppm): 19.0, 19.3, 19.6, 40.2, 60.9, 103.0, 119.0, 120.0, 122.6, 125.1, 125.7, 127.0, 127.5, 127.9, 129.7, 132.1, 132.6, 133.8, 134.7, 134.8, 138.8, 148.5, 149.7, 152.1. Anal. calcd. (%) $C_{27}H_{25}ClN_4$: C, 73.54; H, 5.71; N, 12.71. Found: C, 73.57: H, 5.77, N, 12.93.

### 7-Chloro-N-{4-[5-(benzo[d][1,3]dioxol-5-yl)-4,5-dihydro-1H-pyrazol-3-yl]phenyl} quinolin-4–amine (7j)

Yield: 73.80%. mp: 149–151 °C. IR (KBr pellet $cm^{-1}$): 3215 (NH). $^1$H NMR (270 MHz, δ ppm, DMSO$d_6$): 9.18 (brs, 1H, NH), 8.48 (d, 1H, H2, $J = 5.2$Hz), 8.42 (d, 1H, H5, $J = 9.2$Hz), 7.90 (d, 1H, H8, $J = 1.9$ Hz), 7.66 (d, 2H, H3′, H5′, $J = 8.7$ Hz), 7.58 (dd, 1H, H6, $J = 9.2$Hz, $J =$ 1.97 Hz), 7.36 (d, 2H, H2′, H6′, $J = 8.7$ Hz), 7.01 (d, 1H, H3, $J = 5.2$Hz), 6.94 (s, 1H, H2″), 6.80–6.90 (m, 2H, H5″, H6″), 4.76 (t, 1H, Hb, $J = 10.9$ Hz), 5.98 (s, 2H, H7”), 3.35 (m, 1H, Ha), 2.81 (dd, 1H, Ha, $J = 16.2$Hz, $J = 10.9$ Hz). $^{13}$C NMR (67.9 MHz, δ ppm): 41.2, 64.0, 101.4, 103.0, 107.5, 108.5, 120.3, 122.6, 125.1, 125.3, 125.7, 127.1, 127.9, 128.2, 129.6, 134.7, 137.5, 140.7, 146.9, 147.9, 148.9, 152.2. Anal. calcd. (%) $C_{25}H_{19}ClN_4O_2$: C, 67.80; H, 4.32; N, 12.65. Found: C, 67.83: H, 4.35, N, 12.87.

### 7-Chloro-N-{4-[5-(4-Chlorophenyl)-4,5-dihydro-1H-pyrazol-3-yl]phenyl}quinolin-4–amine (7k)

Yield: 74.70%. mp: 205–206 °C. IR (KBr pellet $cm^{-1}$): 3315. $^1$H NMR (270 MHz, δ ppm, DMSO$d_6$): 9.19 (brs, 1H, NH), 8.49 (d, 1H, H2, $J = 5.2$Hz), 8.42 (d, 1H, H5, $J =$ 9.2Hz), 7.90 (d, 1H, H8, $J = 1.9$ Hz), 7.55–7.66 (m, 5 H, H6, H3′, H5′, H2″, H6″), 7.35–7.45 (m, 4 H, H2′, H6′, H3″, H5″), 7.01 (d, 1H, H3, $J = 5.2$Hz), 4.84 (t, 1H, Hb, $J =$ 10.9 Hz), 3.45 (dd, 1H, Ha, $J = 16.2$Hz, $J = 10.9$ Hz), 2.82 (dd, 1H, Ha, $J = 16.2$Hz, $J = 10.9$ Hz). $^{13}$C NMR (67.9 MHz, δ ppm): 26.1, 40.0, 55.8, 60.7, 99.7, 104.6, 110.6, 117.6, 120.4, 122.0, 123.0, 124.1, 125.3, 127.1, 129.6, 133.5, 135.3, 135.4, 137.0, 147.1, 147.3, 152.7, 155.5. Anal. calcd. (%) $C_{24}H_{18}Cl_2N_4$: C, 66.52; H, 4.19; N, 12.93. Found: C, 66.57; H, 4.22; N, 13.15.

## Biological assays

### Inhibition of β-hematin formation

The assay was performed according to protocols reported (Romero et al. 2018, 2019; Baelmans et al. 2000). A solution of hemin chloride (50 µL, 4 mM), dissolved in DMSO (5.2 mg/mL), was distributed in 96-well micro plates. Different concentrations (100–5 mM) of the compounds, dissolved in DMSO, were added in triplicate in test wells (50 µL). Controls contained either water (50 µL) or DMSO (50 µL). β-hematin formation was initiated by the addition of acetate buffer (100 µL 0.2 M, pH 4.4). The plates were incubated at 37 °C for 48 h to allow for completion of the reaction and centrifuged (4000 RPM × 15 min). The infranatant was washed twice with DMSO (200 µL) and finally, dissolved in NaOH (200 µL, 0.2 N). The solubilized aggregates were diluted 1:2 with NaOH (0.1 N) and absorbances were recorded at 405 nm (Microplate Reader, BIORAD-550). The results were expressed as % IHF.

### Parasite, experimental host, and strain maintenance

Male Balb-C mice, weight 18–22 g, were maintained on a commercial pellet diet at libitum and under conditions approved by Ethics Committee of the Institute of Immunology. A rodent malaria ANKA strain of *Plasmodium berghei*, parasite, was used to infect the animals. Infected erythrocytes, $1 \times 10^6$ erythrocytes diluted in phosphate

buffered saline solution (PBS, 10 mM, pH 7.4, 0.1 mL), were inoculated *ip*. The parasitemia was scrutinized by microscopic examination of Giemsa stained smears (Romero et al. 2018, 2019; Dorn et al. 1998).

### Four-day suppressive test

Caudal vein *i.v* infection of Balb-C mice (18–23 g) was performed with $10^6$ *P. berghei* infected red blood cells ($n = 6$). Two hours after infection, the active in vitro compounds (those that inhibited β-hematin formation) were used for treatment. The active compounds were dissolved in DMSO (0.1 M) and subsequently diluted with Saline-Tween 20 solution (2%) and administered *ip* for 4 days (10 mg $kg^{-1}$). At day 4, the parasite load was assessed by examining Giemsa stained smears. CQ (10 mg $kg^{-1}$) was used as a positive control. Results were expressed as percentage of parasitemia. The survival time of mice infected with *P. berghei* and treated with saline solution was used as base control. Infected not treated mice were used for calculation as a control (Romero et al. 2018, 2019; Peters and Robinson 1999).

### Cell lines

The human cell lines, obtained from American Tissue Culture Collection, Jurkat, Clone E6–1, HL60 and normal lymphocytes purified after standard ficoll hypaque were maintained in culture in RPMI 1640 media supplemented with 10% FBS (Hyclone), 100 U/mL penicillin/0.1 mg/mL streptomycin and 1 mM glutamine (Sigma-Aldrich). The cells were incubated in a humidified atmosphere, at 37 °C, containing 5% $CO_2$ in all the experiments. The experimental assays were performed by culturing $3 \times 10^5$ cells/well with the different compounds in 96 well microtiter plates. Five different assays in triplicate were performed per compound (Romero et al. 2018, 2019).

### Isolation of human totals lymphocytes

Heparinised blood was collected with written consent from healthy human volunteers as specified by the Ethical Committee at the Institute of Immunology. Peripheral blood mononuclear cells (PBMCs) were isolated by density gradient centrifugation using the standard Ficoll-Paque gradient (Histopaque 1077, Sigma, Poole, UK) for 30 min at $500 \times g$. The obtained PBMC was washed twice with RPMI 1640 medium, and cells obtained were resuspended in complete media and counted. Monocytes were depleted by cell adherence to plastic for 1 h at 37 °C. After monocyte depletion, cells were analyzed by flow cytometry. The resulting mononuclear cells were 85% T lymphocytes, 8% B lymphocytes and 7% NK cells. In each of the assays with cell lines, normal lymphocytes were used as a reference. Each experiment was with a different donor. No differences were recorded among donors (Romero et al. 2018, 2019).

### The 3-(4,5-dimethyl-2-thiazolyl)-2,5-diphenyl-2H-tetrazolium bromide (MTT) viability assay

The protocol, a slight modification of Mossmann's MTT protocol (Mosmann 1983), described previously (Suárez et al. 2009), was used to asses cell viability. Briefly, different amount of compounds **4**, **5**, **6**, and **7** (0, 1, 5, 10, 25, 50, 100 µM) were mixed with $5 \times 10^4$ cells/well in 96 well microtiter plates for 24 h. Then, MTT (0.50 mg/mL in PBS) was added to each well, and the plates were incubated for 4 h. The plates were centrifuged at $1800 \times g$ for 5 min, washed, dried, the formazan crystals were solubilized with DMSO, and the plates were read by a microplate reader at 540 nm. $IC_{50}$ was defined as the concentration required to decrease cell viability (formazan crystal formation) by 50% as compared to control, nontreated cells. Cells incubated with CQ, Dox, or $As_2O_3$ were the positive controls of the assay.

### Annexin V/propidium iodide (PI) labeling

Jurkat, Clone E6–1, HL60 cells were treated as indicated, then washed twice with PBS and resuspended in annexin V binding buffer (0.01 M HEPES, 0.14 M NaCl, and 2.5 mM $CaCl_2$). Cells were incubated first with AnnexinV-FITC. Then, with PI (Santa Cruz Biotechnology) as recommended by the manufacturer. The cells were analysed using an Epics XL cytometer (Beckman Coulter). The negative control was untreated cells, and the positive controls were the cells treated with Dox (1 µM), QC (50 µM), or CQ (100 µM) (Romero et al. 2018, 2019; Mijares et al. 2013). Double plots were used to show significant expression of both dyes. Annexin V-FITC (membrane apoptosis), PI (necrosis), the appearance of the two fluorochromes (late apoptosis) and living cells do not express any marker. Normal lymphocytes did not reveal any fluorochrome positiveness up to 5 µM of any of the tested compounds. To compare the effect of the compounds on apoptosis, Dox, QC, and CQ, were used as controls (Romero et al. 2019, 2018; Mijares et al. 2013). The drugs concentration was never higher than 100 µM since DMSO may interfere with the results of the assay. The $IC_{50}$ values of the 12 most active derivatives in both cell lines were: $2.08 \pm 0.10$ to $7.29 \pm 0.86$ µM for HL60 cells, and $2.99 \pm 0.24$ to $11.99 \pm 0.98$ µM for Jurkat cells. Based on these data, apoptosis was assessed at concentrations of 1, 2.5, and 5 µM. The results from 5 µM treatment were shown in the figures.

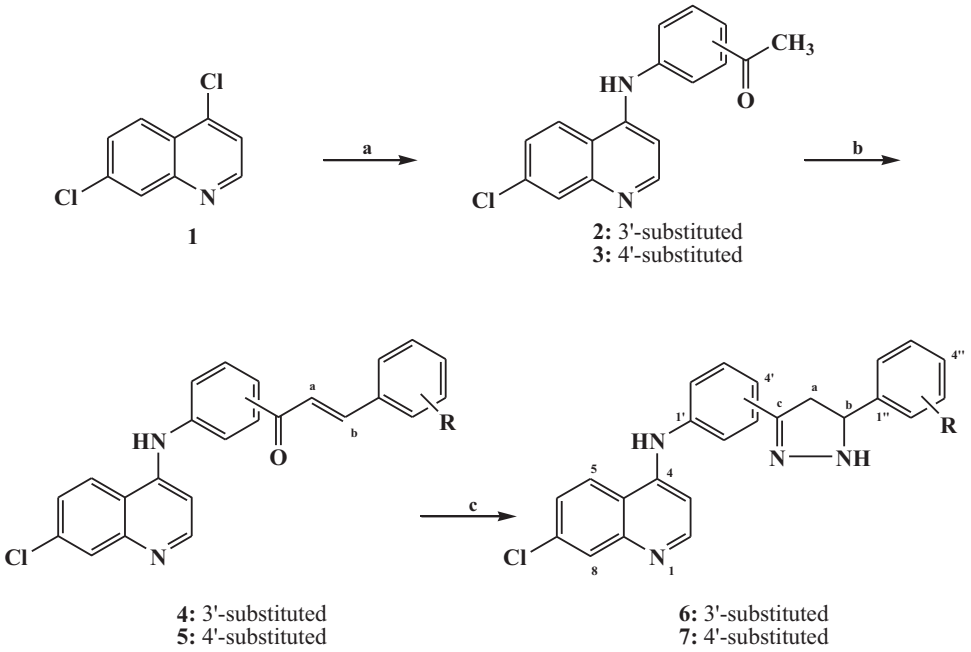


**Scheme 1** Synthesis of quinoline-chalcone and quinoline-pyrazoline hybrids **4**, **5**, **6**, and **7.** Conditions: **a** 3 or 4–aminoacetophenone, EtOH, HCl, Δ, 4 h. **b** substituted benzaldehydes, KOH, MeOH, rt, 72–120 h. **c** hydrazine/$H_2O$, EtOH, Δ, 18–24 h. **R**: **a** 4″ $CH_3$, **b** 2″,3″ $OCH_3$, **c** 2″,4″ $OCH_3$, **d** 2″,5″ $OCH_3$, **e** 3″,4″ $OCH_3$, **f** 3″,5″$OCH_3$, **g** 2″,4″,5″ $OCH_3$, **h** 3″,4″,5″ $OCH_3$, **i** 2″,4″,6″ $OCH_3$, **j** 2″,4″,5″ $CH_3$, **k** 3″,4″-methylenedioxy, and **l** 4″ Cl

### Detection of the expression of the phosphatidylserine by confocal scanning laser microscopy (CSLM)

The HL60 cell line was treated with vehicle, **4c** (1 μM), **4 h** (2.5 μM), Dox (1 μM) and QC (50 μM) by 24 h. Then, the cells were centrifuged and resuspended in 500 μL of annexin binding buffer. Then, 250 ng/ml of annexin V-FITC and 250 ng/ml of PI were added and incubated in the dark for 15 min at room temperature. The detection of phosphatidylserine and PI was monitored in individual cells using a 1 × 81 Olympus inverted microscope with a flow view confocal laser scanning configuration Confocal laser scanning microscopy (CLSM) (Olympus America) equipped with the FV10.ASW program version 02.01.01.04 (Olympus Corporation). The program Imagen Image J (NHI, Washington, DC) was used to process the contrast and brightness of the images.

### Data analysis

One-way ANOVA and *t*-tests for specific group comparisons were used for data analysis. The program used was Graph Pad Prism 3.02 (Graph Pad Prism Software Inc. 1992–2004).

## Results and discussion

### Chemistry

Compounds **2**, **3** were synthesized by adapting an HCl-mediated coupling procedure involving commercial 4,7-dichloroquinoline and an appropriate aniline with a *meta*- or *para*-located acetyl substituent (Ferrer et al. 2009; Insuasty et al. 2013; Romero et al. 2015). The final compounds *(E)*-1-[3 or 4-(7-chloroquinolin-4-ylamino) phenyl]-3-(phenyl substituted) prop-2-ene-1-one **4**, **5** were obtained through aldol condensation of Claisen–Schmidt between **2**, **3** intermediates and differently substituted benzaldehydes (Scheme 1). Only *(E)* isomers were acquired and were confirmed by the coupling constant obtained for the proton–proton coupling in the $^1$H-NMR spectrum. The 7-chloro-*N*-[3 or 4-(4,5-dihydro-5-(phenyl-substituted)-1*H*-pyrazol-3-yl]phenyl quinoline-4–amine **6**, **7** were obtained by a cyclo-condensation reaction with hydrazine monohydrate (Insuasty et al. 2013; Aparicio et al. 2017). The synthesised compounds, obtained in moderate to good yields, were unambiguously characterized by the available spectroscopic techniques.

### Biological

#### Antimalarial activity

All those derivatives were tested in vitro for their effects as inhibitors of β-hematin formation, and in vivo for their efficacy in a murine model (see Table 1). The first mentioned in vitro assay was used to assess the abilities of the derivatives **4**, **5**, **6**, and **7** to inhibit β-hematin formation. In order to evaluate the antimalarial activity, we tested the ability to block heme crystallization, considering that heme can crystallize spontaneously under acid and low oxygen

**Table 1** Percentage of inhibition of β-hematin formation (%IβHF), and effect of quinoline-chalcone and quinoline-pyrazoline hybrids (**4**, **5**, **6**, and **7**) on *P. berghei* infected mice (20 mg/kg)

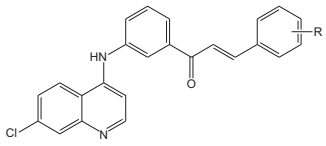


**4a-m**

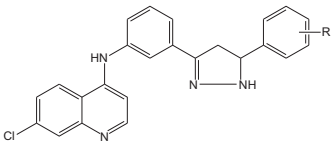


**6e-l**

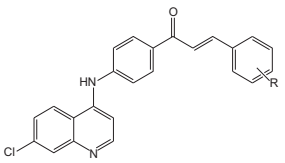


**5a-l**

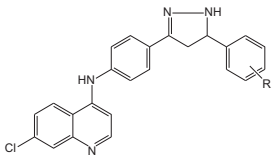


**7c-l**

| No | R | %IβHF(±SD) | Sd(±SD) | %P(±SD) |
|---|---|---|---|---|
| **4a** | 4-$CH_3$ | 54.56 ± 0.03 | nd | nd |
| **4b** | 2,3-$OCH_3$ | 1.22 ± 0.28 | nd | nd |
| **4c** | 2,4-$OCH_3$ | 61.97 ± 0.03 | nd | nd |
| **4d** | 2,5-$OCH_3$ | 44.76 ± 0.21 | nd | nd |
| **4e** | 3,4-$OCH_3$ | 89.73 ± 0.25* | 22.44 ± 2.30† | 1.40 ± 0.89† |
| **4f** | 3,5-$OCH_3$ | 80.66 ± 0.06 | nd | nd |
| **4g** | 2,4,5-$OCH_3$ | 84.24 ± 0.32 | nd | nd |
| **4h** | 3,4,5-$OCH_3$ | 87.75 ± 0.01* | 24.60 ± 2.42† | 1.81 ± 0.46† |
| **4i** | 3,4,5-$CH_3$ | 35.68 ± 0.14 | nd | nd |
| **4j** | –$OCH_2O$– | 31.06 ± 0.02 | nd | nd |
| **4k** | 4-Cl | 94.29 ± 0.02* | 15.80 ± 1.53 | 2.74 ± 0.79 |
| **5a** | 4-$CH_3$ | 85.84 ± 0.16 | nd | nd |
| **5b** | 2,3-$OCH_3$ | 2.97 ± 0.02 | nd | nd |
| **5c** | 2,4-$OCH_3$ | 91.64 ± 0.05* | 14.60 ± 1.47 | 2.27 ± 0.37 |
| **5d** | 2,5-$OCH_3$ | 75.22 ± 0.20 | nd | nd |
| **5e** | 3,4-$OCH_3$ | 86.78 ± 0.03 | 20.31 ± 2.54† | 2.64 ± 0.30† |
| **5f** | 3,5-$OCH_3$ | 14.87 ± 0.27 | nd | nd |
| **5g** | 2,4,5-$OCH_3$ | 90.24 ± 0.01* | 17.43 ± 2.18 | 4.70 ± 0.75 |
| **5h** | 3,4,5-$OCH_3$ | 78.48 ± 0.36 | nd | nd |
| **5i** | 3,4,5-$CH_3$ | 46.26 ± 0.03 | nd | nd |
| **5j** | –$OCH_2O$– | 8.53 ± 0.17 | nd | nd |
| **5k** | 4-Cl | 6.92 ± 0.02 | nd | nd |
| **6e** | 3,4-$OCH_3$ | 91.28 ± 0.08* | 20.57 ± 4.49† | 6.57 ± 1.14† |
| **6f** | 3,5-$OCH_3$ | 91.82 ± 0.08* | 15.17 ± 2.35 | 5.07 ± 0.94 |
| **6g** | 2,4,5-$OCH_3$ | 90.69 ± 0.09* | nd | nd |
| **6h** | 3,4,5-$OCH_3$ | 91.65 ± 0.04* | 12.75 ± 2.02 | 7.15 ± 0.83 |
| **6i** | 3,4,5-$CH_3$ | 17.39 ± 0.19 | nd | nd |
| **6k** | 4-Cl | 83.23 ± 0.20 | nd | nd |
| **7c** | 2,4-$OCH_3$ | 40.63 ± 0.18 | nd | nd |
| **7d** | 2,5-$OCH_3$ | 31.48 ± 0.31 | nd | nd |
| **7e** | 3,4-$OCH_3$ | 9.97 ± 0.51 | nd | nd |
| **7g** | 2,4,5-$OCH_3$ | 89.14 ± 0.12* | 20.23 ± 4.49† | 6.38 ± 1.81† |
| **7h** | 3,4,5-$OCH_3$ | 83.53 ± 0.09 | nd | nd |
| **7i** | 3,4,5-$CH_3$ | 12.75 ± 0.34 | nd | nd |
| **7j** | –$OCH_2O$– | 89.86 ± 0.04* | 13.85 ± 3.19 | 4.77 ± 0.97 |
| **7k** | 4-Cl | 89.21 ± 0.01* | nd | nd |
| **CQ** | – | 98.52 ± 0.01 | 24.99 ± 0.89 | 0.32 ± 0.03 |
| **CiSS** | – | – | 6.80 ± 0.70 | 63.20 ± 0.75 |

$n = 6$

*SD* standard deviation, *Sd* survival days, *%P* percentage of parasitemias, *CQ* chloroquine, *CiSS* control infected and treated with saline solution
*$p > 0.05$ compared to chloroquine. †$p < 0.001$ compared to CiSS

condition found in the vacuole of the parasite (Baelmans et al. 2000). More than 80% of inhibition of heme crystallization were considered significant. Compounds **4e–h**, **k**, **5a**, **c**, **e**, **g**, **6e–h**, **k**, **7g**, **h**, **j**, and **k** were able to inhibit heme crystallization. The values are comparable to CQ (98.52 ± 0.01%). The 3′-phenyl substituted moiety appeared to be favorable for a potential antimalarial activity since most of the combinations showed measurable levels of inhibition of β-hematin formation, except compounds **5a**, **c**, **e**, **g**, **7g**, **h**, **j**. Compound **7k** 4′-phenyl substituted showed good activity. The di or tri methoxy substituted structures in locations (2, 4; 3, 4; 2, 4, 5; 3, 4, 5) or chloride groups in position four of phenyl exhibited excellent activity as inhibitors of β-hematin formation.

The selected compounds that showed a potential antimalarial activity in vitro (**4e**, **h**, **k**, **5c**, **e**, **g**, **6e**, **f**, **h**, **7g**, and **j**) were tested in mice infected with *P. berghei* ANKA a CQ susceptible strain of murine malaria. The antimalarial potential of these compounds was assessed by its ability to reduce parasitemia and increase survival at the fourth-day post-infection as compared to the untreated control group. Mice were treated with compounds (20 mg/kg) or CQ (20 mg/kg) ip once daily for consecutive days (days 1–4 post infection), and their survival times and parasitemia on day 4 were compared with those of control mice receiving only saline (Romero et al. 2018, 2019; Peters and Robinson 1999). The Institute of Immunology Bioethical Committee approved the study according to universal guidelines of the National Research Council's Institute for Laboratory Animal Research (ILAR) and the ethical principles for medical research by the World Medical Association Declaration of Helsinki.

The results are shown in Table 1; the evaluated derivatives can increase the over-exposure of infected mice and reduce parasitemia. Control mice died at 6.80 ± 0.70 days.

Structures **4e** and **h**, used as monotherapy, prolonged the average survival time of infected mice to 22.44 ± 2.30, and 24.60 ± 2.42 days, respectively, but were not able to reduce or delay the evolution of malaria (1.40 ± 0.89 and 1.81 ± 0.46%). CQ prolonged mouse survival time to 24.99 ± 0.89 days and decreased the development of malaria to 0.32 ± 0.03%.

The detailed mechanism by which β-hematin inhibitors obstruct crystal growth is still unknown. It has been proposed that the mechanism of quinoline inhibition is by generating binding to hematin (Egan et al. 1994; Dorn et al. 1998; Egan 2006). Two options are possible: (1) binding to the quickest emergent faces of the β-hematin crystal (Buller et al. 2002; Egan et al. 2001; Pagola et al. 2000), or 2) through a generation of a drug-heme complex covering the hemozoin crystal to impede further crystal growth (Sullivan et al. 1996). Both pathways involve the binding of the compound to Fe(III)PPIX. (de Villiers et al. 2012), have described crystal complexes of quinidine-heme (QD-Fe(III)PPIX) and quinine-heme (QN-Fe(III)PPIX), revealing that three critical interactions are implicated in binding: coordination, hydrogen bonding, and π–π stacking.

In quinine-heme and quinidine-heme structures, there is a hydrogen bond among the propionate group of Fe(III)PPIX and the protonated quinuclidine nitrogen. In addition, (Kelly et al. 2001), using the $^{1}$H NMR technique, documented that the 4,5-dihydroxyxantone-heme complex is stabilized through the hydrogen bonding between the hydroxyl groups and the propionate side chains of the heme, as well as π–π stacking between both aromatic systems. Even though there is no clear information about the requirements for π–π stacking; it was proposed that big planar aromatic molecular surfaces may favor the binding with either hematin of hemozoin.

## Cytotoxic activity

In vitro cytotoxicity of compounds, **4–7** was measured by MTT assay using two different human cancer cell lines: HL60 (acute promyelocytic leukemia), and Jurkat E6.1 (acute lymphocytic leukemia), and human lymphocytes freshly isolated from healthy donors. The Institute of Immunology Bioethical Committee approved the study. Written consent was obtained from each donor.

Doxorubicin, CQ, and $As_2O_3$ were taken as the reference drugs, and the results are summarized in terms of $IC_{50}$ values (see Table 2). Compounds **5a–k** and **7c–j** showed a weak effect against Jurkat E6.1 cell line while against HL60 cell line compounds **5a–k**, **6h**, and **7d–j** showed weak or no activity. A moderate result was observed for compounds **4a**, **c**, **e**, **f**, **i**, **j**, **6e**, **g**, **h**, **k**, and **7k** against the Jurkat E6.1 cell line, while the compounds **4d**, **i–k**, **6k**, and **7c** showed moderate activity against HL60 cells. Compounds **4b**, **d**, **g**, **h**, and **k** exhibit vigorous activity against Jurkat E6.1 cell line. In addition, compounds **4a–c**, **e–h**, **k**, **6e**, and **g** showed vigorous effects as compared with doxorubicin, CQ and $As_2O_3$ against HL60 cell line. The specificity of the compounds was assessed in vitro using normal human lymphocytes. In particular, compounds **4e**, **f**, **6e**, and **g** were less toxic to primary culture human lymphocytes than doxorubicin exhibiting $IC_{50}$ values of >50 and 45.92 ± 3.05 μM, respectively (Table 2). Compounds **4e**, **f**, **6e**, **g** presented a better selectivity index than doxorubicin, being the compounds **4e** > 14 and 25-fold, **4f** > 12 and 17-fold, **6e** 14.5 and 48.9-fold, **6g** > 9.2 and 20.9-fold more selective against Jurkat E6.1 and HL60 cell lines, respectively. This result is remarkable because doxorubicin is one of the most used drugs for cancer treatment.

In order to assess cell death, the cells were cultured for 24 h with the compounds **4–7** and apoptosis was ascertained by flow cytometry. The positiveness of annexin V-FITC and PI was used to define apoptosis or necrosis (Choi et al. 2008),

**Table 2** Effect of quinoline-chalcone and quinoline-pyrazoline hybrids (**4**, **5**, **6**, and **7**) on cell viability (MTT method 1 → 100 μM)

| No | R | Normal lymphocytes | Jurkat E6.1 | HL60 | Selectivity index | Selectivity index |
|---|---|---|---|---|---|---|
| | | | $IC_{50}$(±SD) 24 h | $IC_{50}$(±SD) 24 h | Jurkat E6.1 | HL60 |
| **4a** | 4-$CH_3$ | 15.24 ± 1.02 | 8.05 ± 0.79 | 1.19 ± 0.07 | 1.9 | 12.8 |
| **4b** | 2,3-$OCH_3$ | 7.56 ± 0.36 | 2.27 ± 0.16 | 2.74 ± 0.26 | 3.3 | 2.8 |
| **4c** | 2,4-$OCH_3$ | 8.28 ± 0.85 | 4.00 ± 0.27 | 2.07 ± 0.16 | 2.1 | 4.2 |
| **4d** | 2,5-$OCH_3$ | 10.25 ± 0.66 | 2.93 ± 0.22 | 3.90 ± 0.35 | 3.5 | 4.5 |
| **4e** | 3,4-$OCH_3$ | >50 | 3.44 ± 0.39 | 2.88 ± 0.34 | >14.5 | >25.4 |
| **4f** | 3,5-$OCH_3$ | >50 | 4.16 ± 0.38 | 2.32 ± 0.15 | >12.0 | >17.4 |
| **4g** | 2,4,5-$OCH_3$ | 7.70 ± 0.56 | 2.18 ± 0.17 | 1.08 ± 0.04 | 3.5 | 7.1 |
| **4h** | 3,4,5-$OCH_3$ | 8.09 ± 0.49 | 1.93 ± 0.13 | 2.15 ± 0.12 | 4,.2 | 3.7 |
| **4i** | 3,4,5-$CH_3$ | >50 | 6.17 ± 0.62 | 9.42 ± 0.73 | >8.1 | >5.3 |
| **4j** | –$OCH_2O$– | 15.35 ± 0.92 | 3.58 ± 0.30 | 4.03 ± 0.41 | 4.3 | 3.8 |
| **4k** | 4-Cl | 5.05 ± 0.43 | 2.94 ± 0.34 | 0.59 ± 0.04 | 1.7 | 8.6 |
| **5a** | 4-$CH_3$ | nd | >50 | >50 | nd | nd |
| **5b** | 2,3-$OCH_3$ | nd | 26.35 ± 3.54 | >50 | nd | nd |
| **5c** | 2,4-$OCH_3$ | 35.40 ± 1.86 | 10.36 ± 0.43 | 13.46 ± 1.27 | 3.4 | 2.6 |
| **5d** | 2,5$OCH_3$ | nd | 28.50 ± 2.39 | >100 | nd | nd |
| **5e** | 3,4-$OCH_3$ | >50 | 17.69 ± 1.78 | >100 | >2.8 | >2.0 |
| **5f** | 3,5-$OCH_3$ | nd | >50 | >50 | nd | nd |
| **5g** | 2,4,5-$OCH_3$ | nd | 21.41 ± 3.14 | 50.96 ± 4.21 | nd | nd |
| **5h** | 3,4,5-$OCH_3$ | >50 | 38.28 ± 3.02 | 25.27 ± 1.70 | nd | nd |
| **5i** | 3,4,5-$CH_3$ | nd | >50 | >50 | nd | nd |
| **5j** | –$OCH_2O$– | nd | >50 | >50 | nd | nd |
| **5k** | 4-Cl | nd | >50 | >50 | nd | nd |
| **6e** | 3,4-$OCH_3$ | 45.92 ± 3.05 | 3.17 ± 0.23 | 0.94 ± 0.07 | 14.5 | 48.9 |
| **6g** | 2,4,5-$OCH_3$ | >50 | 5.44 ± 0.55 | 2.39 ± 0.10 | >9.2 | >20.9 |
| **6h** | 3,4,5-$OCH_3$ | >50 | 5.67 ± 0.57 | 12.34 ± 1.07 | >8.8 | >4.1 |
| **6k** | 4-Cl | 41.45 ± 3.44 | 6.92 ± 0.77 | 6.23 ± 0.52 | 6.0 | 6.7 |
| **7c** | 2,4-$OCH_3$ | >50 | 17.89 ± 1.56 | 8.74 ± 0.83 | >2.8 | >5.7 |
| **7d** | 2,5-$OCH_3$ | >50 | 17.56 ± 1.60 | 21.18 ± 1.87 | >2.9 | >2.4 |
| **7g** | 2,4,5-$OCH_3$ | >50 | 23.77 ± 1.11 | 11.34 ± 1.07 | >2.1 | >4.4 |
| **7h** | 3,4,5-$OCH_3$ | >50 | 30.34 ± 2.82 | 19.64 ± 2.24 | >1.7 | >2.6 |
| **7j** | –$OCH_2O$– | 43.82 ± 3.53 | 36.35 ± 1.84 | 22.36 ± 2.12 | 1.2 | 2.0 |
| **7k** | 4-Cl | 48.40 ± 4.51 | 6.31 ± 0.55 | 6.17 ± 0.59 | 7.7 | 7.8 |
| **CQ** | – | >100 | 83.64 ± 8.00 | >100 | >1.2 | >1.0 |
| **Dox** | – | 8.03 ± 0.66 | 1.03 ± 0.18 | 1.60 ± 0.26 | 7.8 | 5.0 |
| **$As_2O_3$** | – | 17.45 ± 1.48 | 7.32 ± 0.61 | 4.97 ± 0.68 | 2.4 | 3.5 |

Data are presented as the mean ± standard deviation of five independent assays. $IC_{50}$ was calculated by non-linear regression (variable slope) analysis using GraphPad Prism

*SD* standard deviation, *Jurkat E6.1* acute lymphocytic leukemia, *HL60* acute myelogenous leukemia, *CQ* chloroquine. *Dox* doxorubicin, *SI* selectivity index tumor cells vs normal lymphocytes, nd not determined

and early or late apoptosis depending on PI expression (early no PI, late annexin V/PI coexpression). Doxorubicin, CQ, and quercetin were taken as the reference drugs (Baran et al. 2010; Chen et al. 2005; Maso et al. 2014; Martínez et al. 2010; Santos et al. 2016; Wei et al. 1994). Figure 1a, b, representsa typical flow cytometry assessment using both cell lines.

Significant differences in the treatments were denoted by the sole increase in annexin V-FITC (early apoptosis). Necrosis, exclusive PI expression, was less prevalent and late apoptosis was observed. The results of all assays are illustrated in Tables S3 and S4 (Supplementary materials).

The expression of annexin V-FITC in the treated cell lines differed. In the 24 h treated HL60 cell line, the

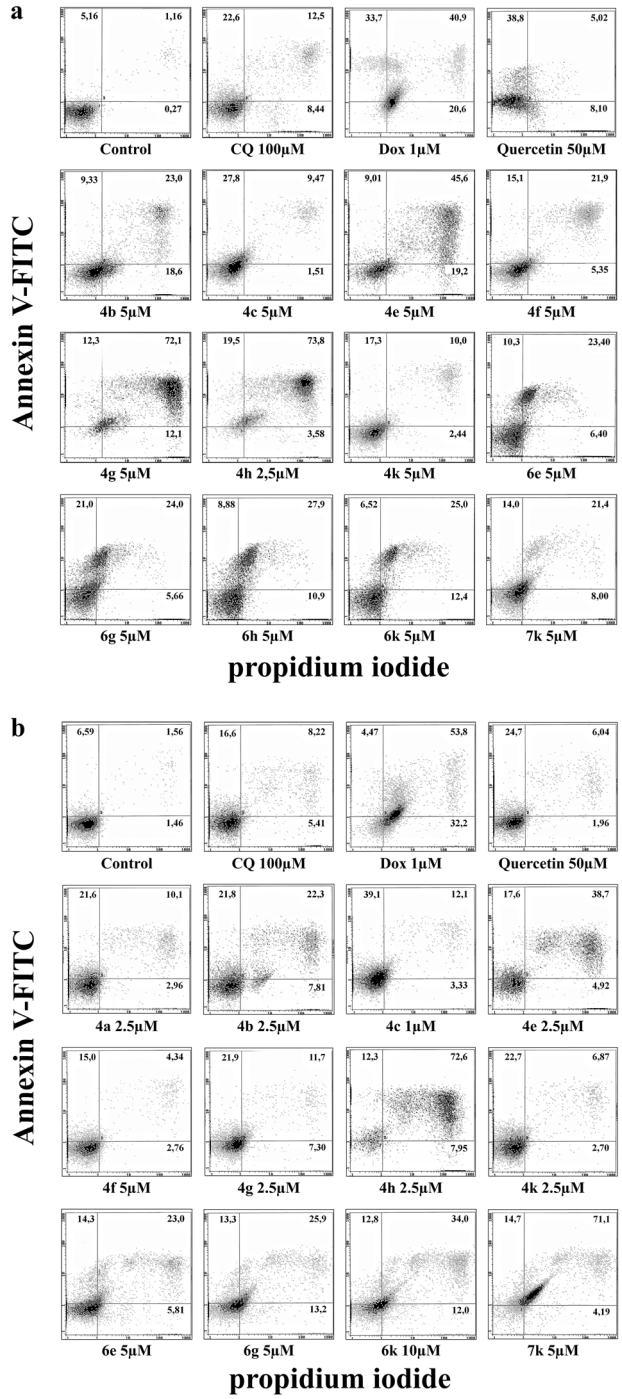


**Fig. 1** **a** Effect of the compounds on apoptosis and necrosis of human Jurkat E6.1 cell line assessed by flow cytometry. Early apoptosis was defined by annexin V-FITC brightness; necrosis expression by PI and late apoptosis by double positiveness. The double plots illustrates the effect of 24 h incubation with compounds **4h** (2.5 μM), **4b**, **c**, **e**, **f**, **g**, **k**, **6e**, **g**, **h**, **k**, **7k** (5 μM), Dox (1 μM), QC (50 μM), CQ (100 μM), and control. Percentages of cells in each quadrant are specified: non-apoptotic alive (lower left), necrotic dead (lower right), early apoptotic (upper left) and late apoptotic (top right). **b** Effect of the compounds on apoptosis and necrosis of human HL-60 cell line assessed by flow cytometry. Early apoptosis is defined by annexin V-FITC expression, necrosis by PI expression and late apoptosis by double positiveness. The double plots illustrates the effect of 24 h incubation with compounds **4c** (1 μM), **4a**, **b**, **e**, **g**, **h**, **k** (2.5 μM); **4f**, **6e**, **g**, **7k** (5 μM), **6k** (10 μM), Dox (1 μM), QC (50 μM) CQ (100 μM), and control. Percentages of cells in each quadrant are specified: nonapoptotic alive (lower left), necrotic dead (lower right), early apoptotic (upper left) and late apoptotic (top right)

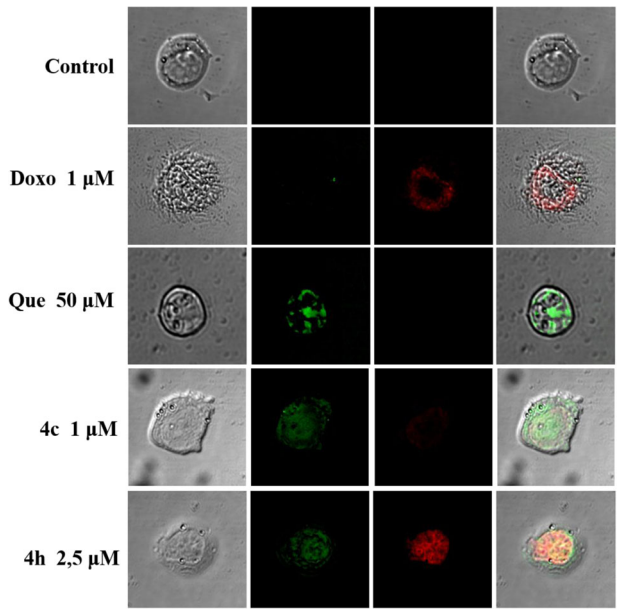


**Fig. 2** Confocal scanning laser microscopy (CSLM) analysis of apoptotic HL60 cells using the PS-binding protein annexin A-FITC and propidium iodide. The HL60 cells were incubated during 24 h with the vehicle (control), **4c** (1 μM), **4h** (2.5 μM), with quercetin (QC) (50 μM), and doxorubicin (Dox) (1 μM), which were used as positive controls. The images are representative of at least three independent experiments; original magnification ×40

maximum effect was reached at concentration range 1–5 μM. At 5 μM, annexin V-FITC expression was 50% or higher in cells treated with compounds **4c** (1 μM), **e**, **h** (2.5 μM), and **7k** (5 μM). The expression was lower than 50% when the cells were treated with the rest of the compounds. On the other hand, annexin V-FITC fluorescence augmented significantly when Jurkat cells were treated with compounds **4e**, **g**, **h**, and **6g**. Compound **4h** was very active; the maximum effect was observed at 2.5 μM in both cell lines. The maximum effect of doxorubicin was recorded at 1 μM. The effects of the compounds on PI expression are illustrated in Tables S3 and S4. The majority of the evaluated compounds did not induce the necrosis in the two cell lines, Fig. 1a, b.

Cell death was ascertained by the expression of annexin V-FITC (green color) and PI (red color) by CSLM, Fig. 2. **4c** and **4h** selection was based on quantitative analysis of percent of apoptotic effect on human Jurkat E6.1 and HL60 cell lines (see Tables S3 and S4). CSLM analysis revealed that the compounds **4c** and **4h** caused a condensation of the

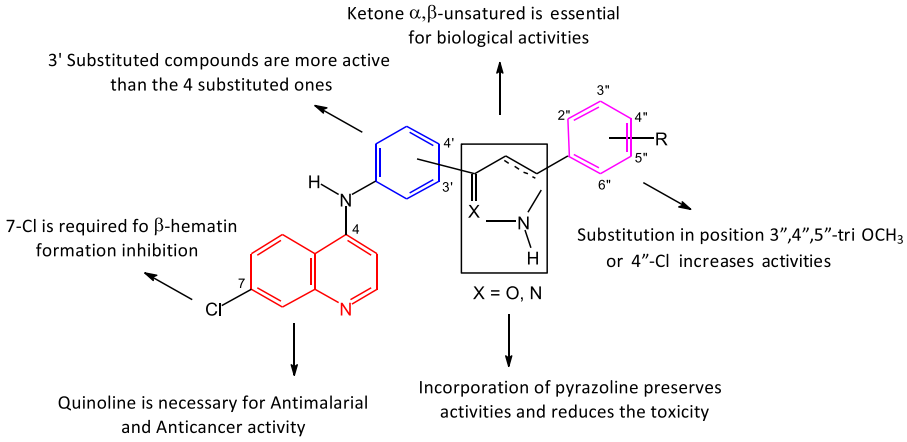


**Fig. 3** Proposed pharmacophoric group based on the bioactivity pattern as antimalarial and anticancer

nuclei and DNA, the formation of vesicles in the membrane, vacuolization, lacerations of the cytoskeleton and formation of apoptotic bodies. The incubation of the HL60 cell line by 24 h with **4c** (1 μM) induced early apoptotic process, as the cells were stained only in green color. In the case of **4h** (2.5 μM), late apoptosis was observed similarly as in flow cytometry experiments. In the case of quercetin (50 μM), which was used as a positive control, there was a predominantly green marking, indicating early apoptosis. Doxorubicin generated a marked increase in cell necrosis.

The green color in Fig. 2 shows the binding, upon expression of phosphatidylserine, while the red color corresponds to the marking of nucleic acids by the PI. The coincidence of both colors (merge) is indicative of late apoptosis only observed with compound **4h** and doxorubicin. However, as previously shown doxorubicin induces cell death in normal lymphocytes also.

## Conclusion

There is a good correlation among inhibition of β-hematin formation, parasitemia reduction, and increase the survival of infected mice with these two most active compounds **4e**, **h**. Our present work demonstrated a possible mechanism of how 4-amino-7-chloroquinoline agents inhibit the β-hematin formation in vivo. Compounds **4e**, **h** could be doing its effect through π–π stacking interaction between the porphyrin ring of the hematin structure and the quinoline ring as it has been reported by CQ and other aminoquinolines (Kumar et al. 2007; Olafson et al. 2015; Goldberg 2013; Kapishnikov et al. 2012). This event would facilitate an active accumulation of the heme/compound complex within the erythrocyte leading to parasite death by oxidative stress. Although these derivatives were active as inhibitors of the β-hematin formation, they were not able to extend the survival rate of infected mice over 25 days. This prolonged survival may be related to pharmacokinetics and the bioavailability of these structures in vivo. Further experiments are required to assess the in vivo mechanism of action.

Compounds **4e**, **f**, **6e**, and **g** showed significant cytotoxic and proapoptotic activity in vitro. These four structures exhibited a better selectivity profile (human leukemia cells vs human lymphocytes). Compound **4h** showed a remarkable in vitro anticancer activity, comparable to the standard drug doxorubicin. In particular, the action of the compound **4h** does not affect the viability of normal human leukocytes at 8 μM, exhibiting a unique activity/toxicity profile.

Our studies demonstrated that compound **4h** could inhibit malaria progression and induction of cell death. The mechanism of action of **4h** in both diseases could be related to the inhibition of heme synthesis and inhibition of lysosome induced autophagy, an effect that has been shown for CQ (Nordstrøm et al. 2015; Bhat et al. 2018; Levy et al. 2017).

Our results are still preliminary and require further analysis especially to *P. falciparum* strains, CQ susceptible and resistant. The following structural features are proposed for the quinoline-chalcone and quinoline-pyrazoline hybrids to be active as antimalarial and anticancer agents (see Fig. 3).

**Acknowledgements** We thank CDCH-UCV (Project PG. 06–8276–2011/2) for financial support.

## Compliance with ethical standards

**Conflict of interest** The authors declare that they have no conflict of interest.

**Publisher's note** Springer Nature remains neutral with regard to jurisdictional claims in published maps and institutional affiliations.

## References

Alegaon S, Parchure P, Araujo L, Salve P, Alagawadi K, Jalalpure S, Kumbarc V (2017) Quinoline-azetidinone hybrids: Synthesis and in vitro antiproliferation activity against Hep G2 and Hep 3B human cell lines. Bioorg Med Chem Lett 27:1566–1571

Aparicio D, Lobo G, Sánchez J, Monasterios M, Acosta M, De Lima L, Llovera L, Angel J, Charris J (2017) Synthesis of trans-and cis-2–acetyl-3–phenyl-3,3a,4,5–tetrahydro-2H-benzo [g]indazoles: evaluation as inhibitors of β-hematin formation. J Chem Res 41:668–672

Baelmans R, Deharo E, Muñoz V, Sauvain M, Ginsburg H (2000) Experimental conditions for testing the inhibitory activity of chloroquine on the formation of beta-hematin. J Exp Parasitol 96:243–248

Baran I, Ganea C, Scordino A, Musumeci F, Barresi V, Tudisco S, Privitera S, Grasso R, Condorelli D, Ursu I, Baran V, Katona E, Mocanu M-M, Gulino M, Ungureanu R, Surcel M, Ursaciuc C (2010) Effects of menadione, hydrogen peroxide, and quercetin on apoptosis and delayed luminescence of human leukemia Jurkat T-cells. Cell Biochem Biophys 58:169–179

Bhat P, Kriel J, Shubha Priya B, Basappa, Shivananju N, Loos B (2018) Modulating autophagy in cancer therapy: advancements and challenges for cancer cell death sensitization. Biochem Pharmacol 147:170–182

Buller R, Peterson M, Almarsson O, Leiserowitz L (2002) Quinoline binding site on malaria pigment crystal: a rational pathway for antimalaria drug design. Crys Growth Des 2:553–562

Cancer Research UK, Worldwide cancer statistics (2018). https://www.cancerresearchuk.org/health-professional/cancer-statistics/worldwide-cancer. (Accessed 03 Aug 2019)

Chen D, Daniel K, Chen M, Kuhn D, Landis-Piwowar K, Dou Q (2005) Dietary flavonoids as proteasome inhibitors and apoptosis inducers in human leukemia cells. Biochem Pharmacol 69:1421–1432

Choi E, Bae S, Ahn W (2008) Antiproliferative effects of quercetin through cell cycle arrest and apoptosis in human breast cancer MDA-MB-453 cells. Arch Pharm Res 31:1281–1285

de Villiers K, Gildenhuys J, Roex T (2012) Iron(III) protoporphyrin IX complexes of the antimalarial cinchona alkaloids quinine and quinidine. ACS Chem Biol 7:666–671

Dorn A, Vippagunta S, Matile H, Bubendorf A, Vennerstrom J, Ridley R (1998) A comparison and analysis of several ways to promote haematin (haem) polymerisation and an assessment of its initiation in vitro. Biochem Pharmacol 55:737–747

Egan T (2006) Interactions of quinoline antimalarials with hematin in solution. J Inorg Biochem 100:916–926

Egan T, Mavuso W, Ncokazi K (2001) The mechanism of β-hematin formation in acetate solution. Parallels between hemozoin formation and biomineralization processes. Biochem 40:204–213

Egan T, Ncokazi K (2005) Quinoline antimalarials decrease the rate of β-hematin formation. J Inorg Biochem 99:1532–1539

Egan T, Ross D, Adams P (1994) Quinoline anti-malarial drugs inhibit spontaneous formation of beta-haematin (malaria pigment). FEBS Lett 352:54–57

Faure E (2016) Puzzling and ambivalent roles of malarial infections in cancer development and progression. Parasitology 143:1811–1823

Ferrer R, Lobo G, Gamboa N, Rodrigues J, Abramjuk C, Jung K, Lein M, Charris J (2009) Synthesis of [(7-Chloroquinolin-4-yl)amino] chalcones: potential antimalarial and anticancer agents. Sci Pharm 77:725–741

Fong K, Wright D (2013) Hemozoin and antimalarial drug discovery. Future Med Chem 5:1437–1450

Goldberg D (2013) Complex nature of malaria parasite hemoglobin degradation. PNAS 110:5283–5284

Graph Pad Prism Software Inc. 4.02 for windows. May 17th (1992–2004).

Grillet M, Hernández-Villena J, Llewellyn M, Paniz-Mondolfi A, Tami A, Vincenti-Gonzalez M, Marquez M, Mogollon-Mendoza A, Hernandez-Pereira C, Plaza-Morr J, Blohm G, Grijalva M, Costales J, Ferguson H, Schwabl P, Hernandez-Castro L, Lamberton P, Streicker D, Haydon D, Miles M, Acosta-Serrano A, Acquattela H, Basañez M, Benaim G, Colmenares L, Conn J, Espinoza R, Freilij H, Graterol-Gil M, Hotez P, Kato H, Lednicky J, Martinez C, Mas-Coma S, Morris Jr. J, Navarro J, Ramirez J, Rodríguez M, Urbina J, Villegas L, Segovia M, Carrasco H, Crainey J, Luz S, Moreno J, Noya-Gonzalez O, Ramírez J, Alarcón-Noya B (2019) Venezuela's humanitarian crisis, resurgence of vector-borne diseases, and implications for spillover in the region. Lancet Infect Dis 19:e149–e161

Handrick R, Ontikatze T, Bauer K, Freier F, Rübel A, Dürig J, Belka C, Jendrossek V (2010) Dihydroartemisinin induces apoptosis by a bak-dependent intrinsic pathway. Mol Cancer Ther 9:2497–2510

Insuasty B, Montoya A, Becerra D, Quiroga J, Abonia R, Robledo S, Vélez I, Upegui Y, Nogueras M, Cobo J (2013) Synthesis of novel analogs of 2–pyrazoline obtained from [(7-Chloroquinolin-4-yl)amino]chalcones and hydrazine as potential antitumor and antimalarial agents. Eur J Med Chem 67:252–262

Joshi A, Viswanathan C (2006) Recent developments in antimalarial drug discovery. Anti-Infect Agents Med Chem 5:105–122

Kapishnikov S, Weiner A, Shimoni E, Guttmann P, Schneider G, Dahan-Pasternak N, Dzikowski R, Leiserewitz L, Elbaum M (2012) Oriented nucleation of hemozoin at the digestive vacuole membrane in *Plasmodium falciparum*. PNAS 109:11188–11193

Kelly J, Winter R, Riscoe M, Peyton D (2001) A spectroscopic investigation of the binding Interactions between 4,5-dihydroxyxanthone and heme. J Inorg Biochem 86:617–625

Kumar A, Srivastava K, Kumar S, Puri S, Chauhan P (2010) Synthesis of new 4–aminoquinolines and quinoline-acridine hybrids as antimalarial agents. Bioorg Med Chem Lett 20:7059–7063

Kumar S, Guha M, Choubey V, Maity P, Bandyopadhyay U (2007) Antimalarial drugs inhibiting. hemozoin (β-hematin) formation: a mechanistic update. Life Sci 80:813–828

Levy J, Towers C, Thorburn A (2017) Targeting autophagy in cancer. Nat Rev Cancer 17:528–542

Lombard M, N'Da D, Breytenbach J, Smith P, Lategan C (2011) Synthesis, in vitro antimalarial and cytotoxicity of artemisinin-aminoquinoline hybrids. Bioorg Med Chem Lett 21:1683–1686

Mahajan A, Yeh S, Nell M, van Rensburg C, Chibale K (2007) Synthesis of new 7-chloroquinolinyl thioureas and their biological investigation as potential antimalarial and anticancer agents. Bioorg Med Chem Lett 17:5683–5685

Maji A (2018) Drug susceptibility testing methods of antimalarial agents. Trop Parasitol 8:70–76

Martínez A, Rajapakse C, Sánchez-Delgado R, Varela-Ramírez A, Lema C, Aguilera R (2010) Arene-Ru(II)-chloroquine complexes interact with DNA, induce apoptosis on human lymphoid cell lines and display low toxicity to normal mammalian cells. J Inorg Biochem 104:967–977

Maso V, Calgarotto A, Franchi G, Nowill A, Filho P, Vassallo J, Olalla S (2014) Multitarget effects of quercetin in leukemia. Cancer Prev Res 12:1240–1250

Meshnick S, Thomas A, Ranz A, Xu C, Pan H (1991) Artemisinin (qinghaosu): the role of intracellular hemin in its mechanism of antimalarial action. Mol Biochem Parasitol 49:181–189

Mijares M, Ochoa M, Barroeta A, Martínez G, Suárez A, Compagnone R, Chirinos P, Avila R, De Sanctis J (2013) Cytotoxic effets of fisturalin-3 and 11-deoxyfisturalin-3 on jurkat and U937 cell lines. Biomed Pap 157:222–226

Mosmann T (1983) Rapid colorimetric assay for cellular growth and survival: Application to proliferation and cytotoxicity assays. J Immunol Methods 65:55–63

Nordstrøm L, Sironi J, Aranda E, Maisonet J, Perez-Soler R, Wu P, Schwartz E (2015) Discovery of autophagy inhibitors with antiproliferative activity in lung and pancreatic cancer cells. ACS Med Chem Lett 6:134–139

Olafson K, Ketchum M, Rimer J, Vekilov P (2015) Mechanisms of hematin crystallization and inhibition by the antimalarial drug chloroquine. PNAS 112:4946–4951

O'Neill P, Barton V, Ward S (2010) The molecular mechanism of action of artemisinin-the debate continues. Molecules 15:1705–1721

Pagola S, Stephens P, Bohle D, Kosar A, Madsen S (2000) The structure of malaria pigment beta-haematin. Nature 404:307–310

Peters W, Robinson B (1999) Parasitic infection models. In: Zak O, Sande M (eds) Handbook of antimalarial models of infection Academic Press, London, p 757

Phillips M, Burrows J, Manyando C, van Huijsduijnen R, van Voorhis W, Wells T (2017) Malaria. Nat Rev Dis Primers 3:17050

Plewes K, Leopold S, Kingston H, Dondorp A (2019) What's new in the management of malaria? Infect Dis Clin N Am 33:39–60

Pretorius S, Breytenbach W, Kock C, Smith P, N'Da D (2013) Synthesis, characterization and antimalarial activity of quinoline–pyrimidine hybrids. Bioorg Med Chem 21:269–277

Ramírez-Prada J, Robledo S, Vélez I, Crespo M, Quiroga J, Abonia R, Montoya A, Svetaz L, Zacchino S, Insuasty B (2017) Synthesis of novel quinoline-based 4,5-dihydro-1H-pyrazoles as potential anticancer, antifungal, antibacterial and antiprotozoal agents. Eur J Med Chem 131:237–254

Ratchanok P, Saekee A, Mandi P, Ch N, Prachayasittikul S, Ruchirawat S, Prachayasittikul V (2014) Synthesis, biological evaluation and molecular docking of novel chalcona-coumarin hybrids as anticancer and antimalarial agents. Eur J Med Chem 85:65–76

Rodrigues J, Charris J, Ferrer R, Gamboa N, Ángel J, Nitzsche B, Hoepfner M, Lein M, Jung K, Abramjuk C (2012) Effect of quinolinyl acrylate derivatives on prostate cancer in vitro and in vivo. Invest New Drugs 30:1426–1433

Romero A, Acosta M, Gamboa N, Charris J, Salazar J, López S (2015) Synthesis, β-hematin inhibition studies and antimalarial evaluation of dehydroxy isotebuquine derivatives against *Plasmodium berghei*. Bioorg Med Chem 23:4755–4762

Romero J, Acosta M, Gamboa N, Mijares M, De Sanctis J, Charris J (2018) Optimization of antimalarial, and anticancer activities of (E)-methyl 2-(7-chloroquinolin-4-ylthio)-3-(4–hydroxyphenyl) acrylate. Bioorg Med Chem 26:815–823

Romero J, Acosta M, Gamboa N, Mijares M, De Sanctis J, Llovera L, Charris J (2019) Synthesis, antimalarial, antiproliferative, and apoptotic activities of benzimidazole-5-carboxamide derivatives. Med Chem Res 28:13–27

Santos G, Almeida M, Antunes L, Bianchi M (2016) Effect of bixin on DNA damage and cell death induced by doxorubicin in HL60 cell line. Hum Exp Toxicol 35:1319–1327

Smit F, N'Da D (2014) Synthesis, in vitro antimalarial activity and cytotoxicity of novel 4–aminoquinolinyl-chalcone amides. Bioorg Med Chem 22:1128–1138

Strasser A, Vaux D (2018) Viewing BCL2 and cell death control from an evolutionary perspective. Cell Death Differ 25:13–20

Suárez A, Chávez K, Mateu E, Compagnone R, Muñoz A, Sojo F, Arvelo F, Mijares M, De Sanctis J (2009) Cytotoxic activity of seco-entkaurenes from Croton caracasana on human cancer cell lines. J Nat Prod Commun 4:1547–1550

Sullivan D, Gluzman I, Russell D, Goldberg D (1996) On the molecular mechanism of chloroquine's antimalarial action. Proc Natl Acad Sci USA 93:11865–11870

Wei Y, Zhao X, Kariya Y, Fukata H, Teshigawara K, Uchida A (1994) Induction of apoptosis by quercetin: involvement of heat shock protein. Cancer Res 54:4952–4957

Weissbuch I, Leiserowitz L (2008) Interplay between malaria, crystalline hemozoin formation, and antimalarial drug action and design. Chem Rev 108:4899–4914

World Health Organization, Media Centre Malaria (2018). http://www.who.int/mediacentre/factsheets/fs094/en/. Accessed 03 Aug 2019

Xu Q, Li Z, Peng H, Sun Z, Cheng R, Ye Z, Li W (2011) Artesunate inhibits growth and induces apoptosis in human osteosarcoma HOS cell line in vitro and in vivo. Zhejiang Univ Sci B 12:247–255

Zhang S, Chen H, Webster J, Gerhard G (2013) Targeting heme for the identification of cytotoxic agents. Anti-Cancer Agents Med Chem 13:515–522

Zhou C, Pan W, Wang X, Chen T (2012) Artesunate induces apoptosis via a bak-mediated caspase-independent intrinsic pathway in human lung adenocarcinoma cells. J Cell Physiol 227:3778–3786